MISSIONE 4
ISTRUZIONE
RICERCA

Hydrothermal versus microbial MEthane release From very shallow coastal systems: can differently sourced emISsions direcTly escape intO the atmosphere? (MEFISTO)

Deliverable 4. Gaseous emission and environmental setting assessment - *Final report of the activities related to WP3*

Laudicella V.A., Caruso C., De Rosa G., De Vittor C., Douss N., Esposito. V., Fonti V., Graziano M., Iacuzzo F., Kralj M., Lazzaro G., Longo M., Relitti F., Retelletti Brogi S., Semprebello A., Bazzaro M.

Finanziato dall'Unione europea NextGenerationEU
Ministero dell'Università e della Ricerca
Italiadomani
OGS

Table of Content

1. SUMMARY 4
2. MEFISTO RESEARCH PROGRAMME AND OBJECTIVES 5
2.1 General scientific background 5
2.2 The MEFISTO project 5
2.3 Volcanic-related CH_4 emissions: the hydrothermal vent system off the Panarea Island (Aeolian Archipelago, Southern Tyrrhenian Sea) 6
2.4 Grébeni/Trezze/Tegnúe: methane-derived deposits in the Northern Adriatic Sea 7
3. MATERIAL AND METHODS 9
3.1. Monitoring plan details 9
3.1.1. CTD-profiling 10
3.1.2. Water column sampling 11
3.1.3. Dissolved gases 12
3.1.4 Spectrophotometric pH on total scale (pHT) and total alkalinity (TA) 13
3.1.5. Major, minor and trace elements 13
3.1.6. Free gas, hydrothermal fluid, interstitial water and sediment sampling 13
3.1.7. Gas efflux at seafloor and gas flux at the air–water interface 14
3.2. Laboratory analyses 14
3.2.1. Carbonate system 14
3.2.2. Other water chemistry parameters 15
3.2.3 Analyses on the sediments: Total organic carbon (TOC) and total sulphur (TS) 16
4. PRELIMINARY RESULTS 17
4.1. Hydrography and CTD profiles from the MEFISTO oceanographic campaigns 17
4.1.1. Physical composition of the water column (salinity and temperature) 17
4.1.2. pH (nbs) and dissolved oxygen over the water column during MEFISTO campaigns in Panarea and Trezze 18
4.2. Patterns in the carbonate system over the four MEFISTO Campaigns 20
4.2.1. Total scale pH referred to the temperature of 25°C (pH_{T25}) 20
4.2.2. Total alkalinity (TA) 21
4.2.3. Dissolved inorganic Carbon (DIC) and comparison with Total dissolved CO_2 (DIC_{DER}) 23
4.2.4. Derived Carbonate system parameters: partial pressure of CO_2 (pCO_2) and Aragonite saturation state (ΩAra) 25
4.3. Other water chemistry parameters 28
4.3.1. Inorganic Nutrients (NUT) 28
4.3.2. Dissolved Organic Carbon (DOC) 29
4.3.3. Dissolved gases in the water column 30
4.3.4. Gas flux at the air–water interface 32
4.3.5. Major ions in the water column 33
4.3.6. Trace elements in the water column 35
4.4. Interstitial fluids composition 37
4.4.1 Major Ions 37

4.4.2. Trace Elements 38
4.5. Sediments elemental composition 41
4.6. Free gases 42
5. ACKNOWLEDGEMENTS 43
6. REFERENCES 44

1. SUMMARY

Following the pre-surveys of the seepage zone off the Marano and Grado lagoon (Northern Adriatic Sea) and the hydrothermal vent area off the Panarea island (Southern Tyrrhenian Sea), which have been accurately described in Deliverables 1-3, this report summarises the field and laboratory activities carried out within the framework of the MEFISTO project to identify the factors that favour or prevent methane release to the atmosphere from twelve sites located in these two shallow Italian coastal systems.
In addition, preliminary results of the hydrological and biogeochemical investigations conducted on the various examined matrices are presented.
The collected data will help to shed light on the dynamics influencing the gaseous emissions from shallow near-shore marine environments by ascertaining possible differences in the water column degassing pathways and fates between microbially sourced and volcanic-related methane emissions. This, in turn, will lead to the achievement of the main goal of the MEFISTO project: to help define the actual contribution of coastal areas to global atmospheric methane, which remains subject to significant uncertainties.

2. MEFISTO RESEARCH PROGRAMME AND OBJECTIVES

2.1 General scientific background

Methane (CH_4), accounting for about 30% of the ongoing atmospheric warming, is today recognized as one of the most powerful greenhouse gases (GHGs), being an even stronger absorber of Earth's emitted thermal infrared radiation than carbon dioxide (Simson, 2021). Atmospheric CH_4 concentrations, which increased by only 700 ppb during the millennium before industrialization, are now more than 2.6 times above estimated pre-industrial equilibrium levels, reaching 1912 ppb in 2022 (Saunois et al., 2025). Such an increase is largely the result of anthropogenic emissions related to human activities, including agriculture, production and utilisation of fossil fuel and waste management practices (Ciais et al., 2014). Nevertheless, since the lifetime of CH_4 in the atmosphere barely exceeds 10 years (Prather et al., 2012), the concentrations and therefore the radiative forcing of this potent GHG are thought to be scaled down in a few decades by just stabilising or reducing the anthropogenic emissions (Shindell et al., 2012). Such an approach is considered an effective and realistic way to rapidly mitigate climate change, making it possible to limit the global temperature rise to 1.5-2.0 °C, as targeted by the Paris Agreement (Nisbet et al., 2019).
In order to verify future emission reductions, a precise quantification of the global CH_4 budget is actually needed but, according to the most recent modelling, important uncertainties still affect the calculations, since global emissions were estimated to range between 576 Tg CH_4 $year^{-1}$ and 737 Tg CH_4 $year^{-1}$ (Saunois et al., 2020). The most important source of uncertainty is attributable to natural emissions, accounting for 40% of the global CH4 budget, 1-13% of which is due to the oceans (Kirschke et al., 2013; Saunois et al., 2016). However, while the open ocean CH_4 emissions are relatively well constrained and are driven by variations that are steadily linked to the organic matter cycling, the global marine flux appears to be mostly influenced by shallow near-shore environments (0-50 mbsl), where CH_4 released from the seafloor can escape to the atmosphere before oxidation (Weber et al., 2019). Here, many forcings can severely affect the amount of CH_4 that reaches the air-sea interface, above all water depth, currents, tides, temperature, water column stratification and microbial methane oxidation (Boles and Clark, 2001; Jordan et al., 2022; Mc Ginnis et al., 2006), but due to limited and scarce data, the actual contribution of coastal areas to atmospheric CH_4 is still quite uncertain (Weber et al., 2019).

2.2 The MEFISTO project

The MEFISTO project aims to reduce the abovementioned uncertainties in the estimates of the natural CH_4 fluxes by providing new data on the emissions from shallow near-shore marine environments, where, rapidly bypassing the water column by bubble transport, this powerful GHG can be directly released into the atmosphere (Weber et al., 2019). The lack of data on CH_4 fluxes in coastal areas has significant implications for the accurate calculation of the atmospheric budget for this gas and the accuracy of this estimate is crucial for verifying potential emission reductions associated with the adoption of effective climate change mitigation strategies. The MEFISTO

project, combining classical physical, chemical, and molecular methods with innovative hydroacoustic approaches, will help to fill this knowledge gap by focusing on the study of two Italian shallow coastal areas: a seepage zone recently identified in the Gulf of Trieste, centred on the Bardelli outcrop (Northern Adriatic Sea) and the hydrothermal vent area off the Panarea Island (Aeolian Archipelago, Southern Tyrrhenian Sea).
The project has three main objectives: 1) to ascertain possible differences in the water column degassing pathways and fates between microbially sourced and volcanic-related CH_4 emissions; 2) to assess the main physical and biological forcings (i.e., water depth, currents, tides, temperature, water column stratification and microbial community structure and composition) favouring or preventing the release of CH_4 to the atmosphere from the two investigated marine shallow areas; 3) to eventually develop local emission estimates that will contribute to the refinement of the global atmospheric CH_4 budget.

2.3 Volcanic-related CH_4 emissions: the hydrothermal vent system off the Panarea Island (Aeolian Archipelago, Southern Tyrrhenian Sea)

The Aeolian Archipelago is the expression of the volcanism migrating south-eastward from the Central and Southern Tyrrhenian Sea during the Lower Pleistocene. Submarine emissions of CO_2-rich gases and thermal water outflow is documented in this area since the Roman Age (De Astis et al., 2003). The archipelago includes the active volcanoes of Stromboli, Vulcano, Lipari and Salina. Panarea is the smallest among the Aeolian Islands and represents the subaerial portion of a 2000 m high and 20 km wide submarine stratovolcano, a dormant edifice with a known age range of ca. 150-200 ka (Anzidei et al., 2005; Calanchi et al., 1999; Dolfi et al., 2007).
As a matter of fact, Panarea volcano was generally considered extinct until November 3, 2002, when a low-energy submarine explosion, due to the injection of magmatic fluids in the deep geothermal body (Caracusi et al., 2005), caused an intense and long-lasting submarine gas eruption in the ~2.3 km^2 area rimmed by the islets of Lisca Bianca, Bottaro, Lisca Nera, Dattilo, and Panarelli, about 2.5 km east of Panarea, leading to the opening of a submarine crater 20x8 m wide and 9 m deep (Anzidei and Esposito, 2003; Anzidei et al. 2005; Esposito et al. 2006; Figure 2.1).
The explosion released a huge amount of CO_2 that provoked a drop of seawater pH to a value of 5.6-5.7 and the “degassing crisis” lasted several months (Caracusi et al., 2005; Romano et al., 2019).
Several studies conducted in the islet area indicated that, with about 98% CO_2, the composition of the persistent gaseous emissions is quite stable (Beaubien et al., 2014; Caliro et al., 2004; Espa et al., 2010; Marchini et al., 2021; Sani et al., 2024). Nevertheless, CH_4 concentrations, showed values up to 900 ppm, are generally not negligible (Romano et al., 2019), making the islet area of Panarea suitable for the MEFISTO project purposes.

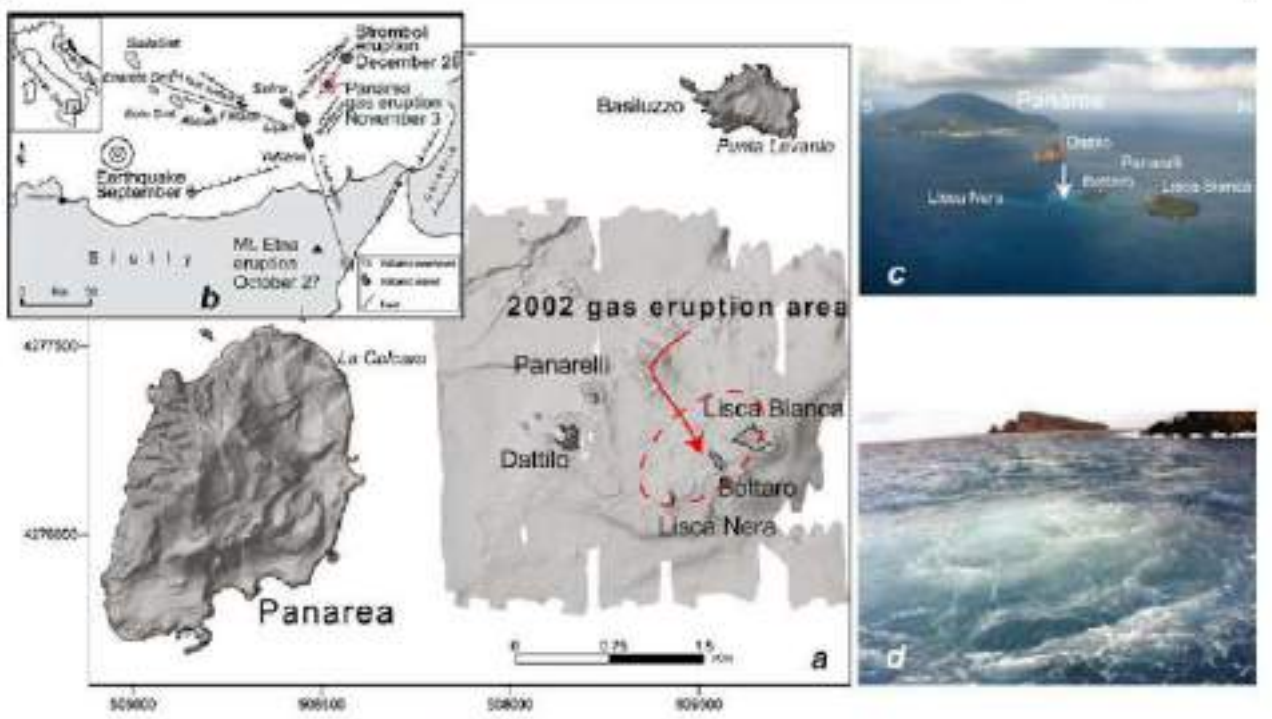

Figure 2.1. a) Location of the 2002 gas eruption. b) Structural sketch map of the Southern Tyrrhenian Sea and Aeolian Islands. c) Aerial view of Panarea Island and islet area with indication of major emission point. d) Gas bubbling in sea surface above the Bottaro crater. From Esposito et al. (2010).

2.4 Grébeni/Trezze/Tegnúe: methane-derived deposits in the Northern Adriatic Sea

The Northern Adriatic Sea is generally characterized by a rather monotonous seabed, consisting mostly of mobile silty-sandy sediments. Nevertheless, numerous submarine rocky substrates of biogenic concretions, called “grébeni” or “trezze” in the Gulf of Trieste and “tegnúe” off the coast of Venice, are irregularly scattered over the soft bottom of this Adriatic Sea sub-basin (Casellato and Stefanon, 2008; Ingrosso et al., 2018; Lipej et al., 2016). Their size ranges from a single small block of 1 m^2 up to a few 1000 m^2, and their height rarely exceeds 4 m. These rocky substrates are suitable for the settlement and development of specific floristic and faunistic assemblages, that are favoured by the accumulation of calcareous incrusting algae, creating complex biostructures commonly referred to as “coralligenous” and giving the colourful underwater landscape a typical appearance (Lipej et al., 2016; Turicchia et al., 2022).

For this reason, since 2015, a limited number of biogenic outcrops in the Gulf of Trieste have been legally protected under the European Habitats Directive (92/43/EEC) and included in the European Natura 2000 network as Sites of Community Importance (Decision EU 2015/69 of December 3, 2014) (Bettoso et al., 2023). These sites are generally called “IT3330009 - Trezze San Pietro e Bardelli” (Figure 2.2).

Up to 4000 outcrops are currently recorded in the Northern Adriatic Sea (Figure 2.1), mostly off the Venetian coast, while in the Gulf of Trieste about 250 have been mapped so far, most of them off the lagoon of Marano and Grado, at a distance of 3 to 10 nautical miles (nm) from the coast and at a depth ranging between 13 and 25 m (Caressa et al., 2001).

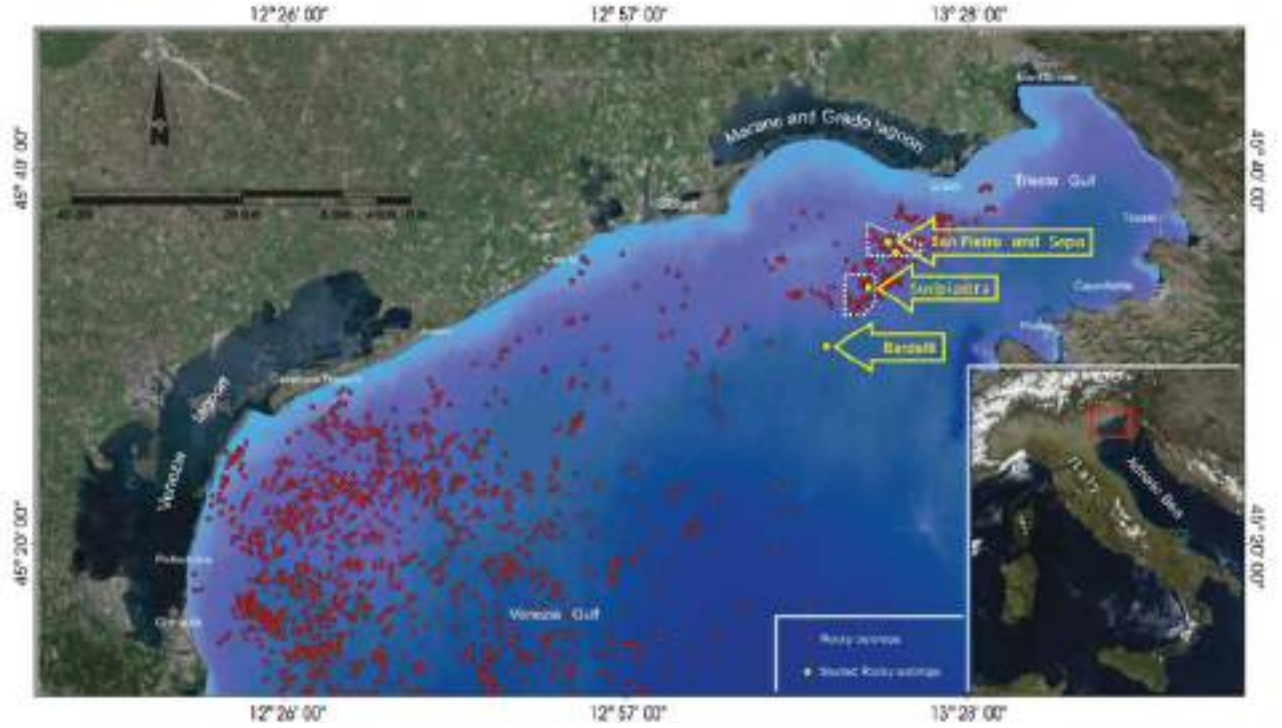

Figure 2.2. Location map of the northern Adriatic Sea rock outcrops (red dots) where the position of trezze San Pietro, Sepa, Sudpiastra and Bardelli is highlighted. Sites of Community Importance in the Gulf of Trieste are indicated by white dashed polygons (mod. from Gordini et al., 2012).

These coralligenous buildups are often associated with gas seeps, thus leading to interpret such deposits as methane-derived carbonates. In fact, several gas fields were discovered and exploited during the 1960s in the Northern Adriatic Sea, where, particularly in the averagely 22 m deep Gulf of Trieste, gas seeps can produce up to 20 m-high gas flares and intermittent bubbling within the water column (Donda et al., 2019; Gordini et al., 2012). These seep gases, mainly composed of CH_4 and occurring both in deep and shallow Plio-Quaternary successions, are microbial in origin and mostly originate from laterally persistent Late Pleistocene peat layers, which are widely distributed throughout the Northern Adriatic Sea and represent the main source of organic matter feeding the gases (Donda et al., 2019).

3. MATERIAL AND METHODS

3.1. Monitoring plan details

The four sampling campaigns foreseen by the MEFISTO project have been carried out between March 2024 and April 2025. For Panarea island the first campaign - under winter conditions - was completed between 21st and 23rd March 2024, while the second campaign, which aimed to capture a snapshot of the summer gas dynamics and environmental setting in the area, was conducted between September 26-28th 2024. Both campaigns have been carried out on board the M/N Corvo and thanks to the support of the Panarea Natlab Italy facility (operated by OGS).

Figure 3.1 Vessels supporting the project activities during the four MEFISTO campaigns: M/N Corvo (top) operating off Panarea island and M/N Castorino 2 (bottom) operating on the “trezze” off the Marano and Grado lagoon.

The campaigns in the "Trezze" of the Northern Adriatic Sea were instead completed between July 2024 and April 2025. The first campaign, snapshotting the sites under summer conditions, was done between 16th and 18th July 2024, whereas the second campaign was conducted between April 7th-10th 2025, sampling the various sites during winter conditions. Both samplings were carried out with the logistic support of M/N Castorino 2, Shoreline soc. cop. and the Grado Coast Guard.
All the sites monitored have been selected following a literature records search and visual inspection of the study sites by a remote operated vehicle (ROV) or scuba divers. Full reports of the site selection procedures are available in MEFISTO Deliverable 1-3. The full list of sampling sites with geographical coordinates are available in table 3.1.

Table 3.1 - Stations investigated in the Northern Adriatic Sea and Southern Thyrrenian Sea in the framework of the MEFISTO project.

Area	*Station*	*Depth (m)*	*Longitude (Degree Minutes)*	*Latitude (Degree Minutes)*
Panarea - Southern Thyrrenian Sea	Black Point Smoke	21.0	15°06.630' E	38°38.217' N
Panarea - Southern Thyrrenian Sea	Black Point Bubbling	21.0	15°06.630' E	38°38.217' N
Panarea - Southern Thyrrenian Sea	Bottaro Twins	6.25	15°06.623' E	38°38.324' N
Panarea - Southern Thyrrenian Sea	Bottaro Single	6.25	15°06.623' E	38°38.324' N
Panarea - Southern Thyrrenian Sea	Bottaro Downstream	4.0	15°06.648' E	38°38.320' N
Panarea - Southern Thyrrenian Sea	Hot/Cold1	10.0	15°04.704' E	38°38.553' N
Panarea - Southern Thyrrenian Sea	Hot/Cold2	11.3	15°04.653' E	38°38.280' N
Panarea - Southern Thyrrenian Sea	Zimmari	8.5	15°03.969' E	38°37.589' N
Trezze - Northern Adriatic Sea	San Pietro	14.0	13°20.276 E	45°36.191 N
Trezze - Northern Adriatic Se	Sepa	16.7	13°20.581 E	45°35.622 N
Trezze - Northern Adriatic Se	Sudpiastra	19.0	13°18.305 E	45°33.218 N
Trezze - Northern Adriatic Se	Bianco	15.5	13°16.721 E	45°34.652 N

3.1.1. CTD-profiling

During the four MEFISTO campaigns, hydrographic data were obtained by means of a Conductivity-Temperature-Depth probes (CTD) provided by the OGS ECCSEL Natlab Italy laboratory of Panarea and the OGS TEC infrastructure (Section of Oceanography). During the Panarea campaigns (March 2024 and September 2024) a multi-parametric probe (RBRmaestro³) equipped with a multi-channel logger (for conductivity, temperature, pressure, dissolved oxygen and pH detection), a CONTROS HydroC CO_2 and a CONTROS HydroC CH_4 sensors was employed. A multiparametric CTD probe SBE19plus V2 (Sea-bird Scientific) equipped with a pH probe (SBE18, Sea-bird Scientific), a fluorimeter/turbidimeter probe (ECO-FLNTU, Sea-bird Scientific) and a dissolved oxygen sensor (SBE43, Sea-bird Scientific) was instead employed during the two campaigns in the North Adriatic "Trezze" sites (July 2024 and April 2025).

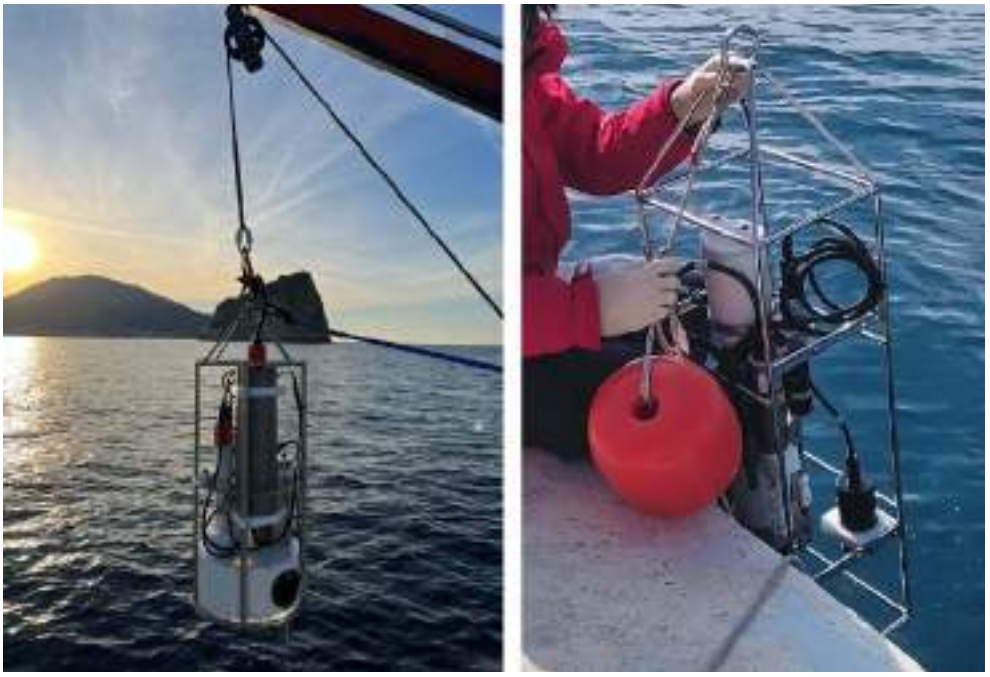

Figure 3.2 Multiparametric probes employed during the project field activities. On the left: RBRmaestro equipped with a multichannel logger and CONTROS Hydroc CO_2 and CONTROS Hydroc CH_4 sensors. On the right: SBE19plus V" equipped with pH, fluorometer/turbidimeter and dissolved oxygen sensors.

3.1.2. Water column sampling

At each site, discrete water samples were collected along the water column at different depths (i.e., Surface – SUR, Intermediate – INT, and Bottom – BOT for sites with depth >10 m, and Surface – SUR and Bottom – BOT for sites with depth <10 m) using a grapnel consisting of three Niskin bottles closed at each depth (Fig. 3.3). Scuba divers were responsible for positioning and closing the grapnel at the bottom near the emission sites. Bottom depth and seawater temperature for bottom samples were obtained from consensus between the scuba divers' diving computers and CDT cast profiles made on site.

Once on board, the three Niskin bottles for each depth were immediately processed to sample various biotic and abiotic parameters. One bottle was used entirely for prokaryotic community and metagenomic analyses (see Deliverable 5 for further details), while the remaining two bottles were processed for water chemistry.

The sequence and procedures for sampling water chemistry parameters followed the principles and standard operating protocols described in the GO-Ship Hydro Manual.

Priority was given to dissolved gases and related parameters such as dissolved oxygen (DO) (assessed during the two Panarea sampling campaigns), dissolved inorganic carbon (DIC), and pH, following Standard Operating Procedure (SOP) 1 (Dickson et al., 2007a), to minimise sample degassing. DO was sampled according to the amperometric Winkler method (Langdon, 2010), DIC was collected according to SOP 2 (Dickson et al., 2007b), and pH and total alkalinity (TA) were processed according to SOP 6b and SOP 3b, respectively (Dickson et al., 2007d–c). Samples for dissolved inorganic nutrients (nitrite – NO_2, nitrate – NO_3, ammonium – NH_4, phosphate – PO_4, and

silicate – $Si(OH)_4$) were filtered on board with pre-combusted Whatman GF/F filters (450 °C for 4 h) in acid-washed polyethylene vials rinsed with seawater sample and kept frozen (−20 °C) until laboratory analysis (Becker et al., 2020).

Figure 3.3. Deployment of Niskin bottles in “Bottaro Twins”.

3.1.3. Dissolved gases

From the Niskin bottles collected at each layer, subsampling was carried out for onshore analysis of dissolved gases, major components, and trace elements. Once all physico-chemical parameters such as temperature, electrical conductivity, pH, and Eh were measured, three 160 ml glass vials were filled to determine dissolved gas compositions by gas chromatography using the headspace method described in section 3.2.2.3. Vials were filled via a silicone tube connected to the Niskin bottle. The silicone tube was placed at the bottom of the vial to completely fill it with seawater, displacing all air and avoiding degassing. Once the vial was filled, it was completely submerged in seawater from the same Niskin bottle, keeping the silicone tube at the bottom and allowing the sample to overflow. The tube was then slowly removed, taking care to avoid any air bubbles, and the vial was sealed with a PTFE septum using special crimping pliers. No preservants were added to the water sample to stop possible microbial activity.

For DO, samples were collected from the Niskin bottle with a small silicone tube directly into 125 ml oxygen flasks (Pyrex Erlenmeyer 125 ml flasks with flared necks and ground glass stoppers) previously volume-tared to ± 0.003 ml. DO in the sample was fixed by adding 0.3 ml of manganous chloride ($MnCl_2$) solution and 0.3 ml of an alkaline sodium hydroxide-sodium iodide solution (NaOH/NaI). The stopper was then placed on the flask, taking care to avoid entrapping air, vigorously shaken, and stored in a dark, cool place. DO samples were then analysed in the laboratory within 24 hours of sampling by potentiometric titration with sodium thiosulphate (0.01 M) using an iodine (KI, Osil) standard calibration curve with an automatic titrator (G20, Mettler Toledo) equipped with a pH probe (DGi140-SC, Mettler Toledo) according to Langdon, 2010.

For DIC, water samples were collected from the Niskin's bottle into 40 ml borosilicate vials, spiked with 0.05 ml of a 50% $HgCl_2$ solution and stored at 4°C in the dark until analysis (Dickson et al., 2007b).

3.1.4 Spectrophotometric pH on total scale (pH_T) and total alkalinity (TA)

SOP 6b recommends immediate pH analysis after sampling, which during the Panarea campaigns was possible due to the instrumentation available at the ECCSEL Panarea Natlab, Italy, operated by OGS. For pH measurements, samples were collected directly in situ from the Niskin bottle using silicone tubing (internal diameter 0.2 cm), into 10 cm pathlength cylindrical quartz spectrophotometric cells (Starna Scientific), taking care to not leave headspace. These were stored in a dark, cool place and analysed immediately using a spectrophotometer (Varian Cary 60, Agilent Technologies), as detailed in section 3.2.1. During the "Trezze" sampling campaigns, due to logistical reasons (distance from the laboratory and other time constraints), same-day spectrophotometric pH analysis was not feasible. Therefore, pH samples were collected together with TA samples and subsampled for pH analysis directly in the laboratory. This procedure was also applied to Panarea samples to ensure consistency in the analysis. In this case, water samples were collected into 250 ml screw-cap borosilicate bottles (Wheaton, UK), leaving 1% headspace. The caps of these bottles have a Teflon insert to prevent gas exchange or losses during storage. Each sample was spiked with 100 µL of a saturated $HgCl_2$ solution (approximately 8 g L^{-1} in Milli-Q water, Dickson et al., 2007c) and stored in the dark at 4 °C until analysis.
pH was subsampled and analysed within one month from sampling date. TA/pH and DIC samples from Trezze were filtered through pre-combusted GF/F (Merck Millipore) filters, as indicated by Bockmon and Dickson 2014 to remove phytoplankton cells and $CaCO_3$ particles derived from the karstic watershed or calcifying organisms, which could artificially alter TA during titration.

3.1.5. Major, minor and trace elements

Directly from the silicone tube connected to the Niskin bottle samples for major chemicals determinations by mean of liquid chromatography, were collected by filling 50 ml pTE bottle with filtered water (0.45 µm) devoted to anions determinations, 50 ml pTE bottle with filtered (0.45 µm) and acidified water devoted to cations. Major and trace elements were analysed in the water column and in the interstitial/hydrothermal fluid samples.

3.1.6. Free gas, hydrothermal fluid, interstitial water and sediment sampling

Scuba divers were also responsible for collecting free gas, hydrothermal fluid, interstitial water and sediment samples. Free gases were collected for subsequent gas chromatography analysis by positioning a plastic inverted funnel directly above the emission point, connected to an upside-down vial previously filled with seawater. The gas emission displaced the seawater from the vial until only gas remained in the container directly above the emission points. The gas compositions were determined as detailed in section 3.2.2.3. Additionally, for major chemicals and trace elements, interstitial water circulating within the top 10 cm of sediments near the emission point was

collected. A Teflon probe with millimetric holes at its tip was inserted into the sediment to completely fill a 250 ml PTE sampler, using a three-way valve and a 100 ml syringe to draw water directly from the sediment and then transfer it into the bottle until it was completely filled.

3.1.7. Gas efflux at seafloor and gas flux at the air–water interface

Gas efflux at the seafloor was measured using hydrophones deployed by divers near the emission points (see *Deliverable 7. Conceptual and quantitative CH4 emission models – Final Report of the activities related to WP5*). Furthermore, floating chambers were used to determine the vertical gas flux at the air–water interface by calculating the concentration increase within the chamber during the measurement period.

3.2. Laboratory analyses

Once in the laboratory the water samples were appropriately stored awaiting to be analysed. Water samples were assessed for carbonate system parameters (TA, pHT and DIC), the samples were stored at 4°C in darkness and analysed within 3 months from collection (one month in case of pH). Water samples for nutrient analysis (NUT) and solid matrices (sediments and biofilm) for total organic carbon (TOC) and total sulfur (TS) analyses were instead stored in a freezer at -20°C. Further analyses conducted for water and interstitial/hydrothermal fluid samples included dissolved gases, major ion composition and trace element analyses. The following sections will detail the analytical procedures employed for each parameter.

3.2.1. Carbonate system

Three parameters were considered during the MEFISTO campaigns as carbonate system descriptors: spectrophotometric pH, total alkalinity (TA), and dissolved inorganic carbon (DIC).
The pH, reported on the total scale (pHT), was measured using the spectrophotometric method (Dickson et al., 2007d) with purified meta-cresol purple dye, following the method of Liu et al., 2011. When pH was subsampled from TA bottles (see section 3.1.4 for details), the water sample was gently siphoned from the bottle via silicone tubing (internal diameter 0.2 cm) into 10 cm pathlength cylindrical quartz spectrophotometric cells (Starna Scientific), leaving no headspace. All samples were acclimated to 25°C in the dark before analysis. The analysis was performed on a thermostated double light path Varian Cary 100 (Agilent Technologies) equipped with a thermostatic chiller (EcoSilver, Lauda). The analytical temperature was set to 25°C, and the analytical precision was estimated at ±0.003 pHT units, determined from replicate sample analysis, analysis of CO_2 reference material (Batch #209, provided by A.G. Dickson, Scripps Institution of Oceanography, University of California San Diego), and from intercalibration and proficiency exercises (OA-MEDeu intercalibration exercise; WePal Quasimeme).
Total alkalinity (TA) was determined by two-stage potentiometric titration in an open cell (Dickson et al., 2007c) with an automatic titrator (G20, Mettler Toledo) equipped with a glass pH probe (DGI115-SC, Mettler Toledo). The HCl titrant solution (0.1 mol kg^{-1}) was prepared in a NaCl background (0.66 M) to match the ionic strength of the seawater samples, and calibrated against

certified reference seawater (Batch #209, provided by A.G. Dickson, Scripps Institution of Oceanography, University of California San Diego) and in-house quality control samples (replicate seawater samples and standard alkalinity solutions prepared with $NaHCO_3$ secondary standard grade - Sigma Aldrich and processed according to Dickson et al., 2007c). Approximately 100 g of sample was weighed with an analytical scale (0.01 g precision), then transferred to a jacketed beaker in which the sample temperature was stabilised to 25°C before titration. TA was calculated from titration data using a non-linear least squares approach, following the instructions and Excel spreadsheet provided by Curry et al., 2024.

Instrumental DIC was determined using a Shimadzu TOC-V CSH analyser. For DIC, samples were injected into the instrument port and directly acidified with H_3PO_4 (25%), and the generated CO_2 was carried to a nondispersive infrared detector (NDIR). Analysis showed a coefficient of variation <2%. The reproducibility of the method was between 1.5% and 3%.
From DIC and TA, with the integration of salinity and inorganic nutrients, carbonate system parameters were derived using CO2Sys v3.0 software (Pierrot et al., 2021), employing the following coefficients and constants:

- K_1, K_2 from Mehrbach et al., 1973, refit by Dickson and Millero, 1987
- $KHSO_4$ from Dickson, 1990
- KHF from Perez and Fraga, 1987
- pH Scale: Total scale (mol/kg-SW)
- $[B]_T$ Value: Lee et al., 2010

The derived parameters included total dissolved CO_2 (DICder), partial pressure of CO_2 (pCO_2), and aragonite saturation state (Ωara).

3.2.2. Other water chemistry parameters

3.2.2.1. Inorganic nutrients

The analyses of dissolved inorganic nutrients (nitrite – NO_2, nitrate – NO_3, ammonium – NH_4, phosphate – PO_4, and silicate – $Si(OH)_4$) were carried out according to Grasshoff et al. (1999a, 1999b) using a four-channel continuous flow analyser QuAAtro (Seal Analytical Inc., Mequon, WI, USA) AutoAnalyzer. Detection limits were 0.01, 0.02, 0.02, 0.01, and 0.03 µmol L^{-1} for NO_2, NO_3, NH_4, PO_4, and $Si(OH)_4$, respectively.

3.2.2.2. Dissolved Organic Carbon (DOC)

For DOC analysis, water samples were previously acidified (automatically into instrument syringe, 2%-6 M HCl) and after CO_2 elimination, the concentration was determined using a high temperature catalytic method (Sugimura and Suzuki 1988). Samples were then combusted on a catalyst bed at 680 °C and the generated CO_2 was analysed via a nondispersive infrared detector

(NDIR). Analysis showed a variation coefficient <2 %. The reproducibility of the method was between 1.5 and 3 %.

3.2.2.3. Dissolved gases, major and trace elements

The method used in dissolved gas analysis is based on the equilibrium partitioning of gas species between a liquid and a gas phase after introducing a host gas (Ar) into the sample, as shown by Capasso and Inguaggiato 1998, Inguaggiato and Rizzo 2004 and Italiano et al. 2009. The analysis was carried out in the INGV-Palermo laboratories using a gas chromatograph (Agilent 7890) equipped with a double detector (a thermal conductivity detector - TCD and a flame ionisation detector - FID with a methaniser) and Ar as the carrier gas. H_2, O_2, N_2 and CO_2 were measured with the TCD, while CH_4 and CO were determined with the FID coupled to the methaniser. Standard mixtures were routinely analysed before each analytical session, and analytical precision was always better than 5%.
Major elements were analysed in the INGV-Palermo laboratory using ion chromatography systems (Dionex-Thermo ICS 1100) in suppressed mode, equipped with an AS14A column and AG14A precolumn for anions (F^-, Cl^-, Br^-, and SO_4^{2-}), and a CS12A column and CG12A precolumn for cations (Li^+, Na^+, K^+, Mg^{2+} and Ca^{2+}). The columns operate under a continuous flow of carbonate–bicarbonate eluent for anions and methanesulphonic acid eluent for cations. The precision and accuracy of the method are typically better than 5%. During each analytical session, a certified material was analysed to check accuracy.
Trace element concentrations (Li, B, Al, Ti, V, Cr, Mn, Fe, Co, Ni, Cu, Zn, As, Sr, Ba and Pb) were determined in the INGV-Palermo laboratory using an ICP-MS instrument (Agilent 7800). The concentrations of the elements in the samples were calculated with the spectrometer software (ICP Expert version 7.6, Agilent). The precision (RSD, relative standard deviation) of the analysis was calculated from five repetitions for each sample and was always better than 10%.

3.2.3 Analyses on the sediments: Total organic carbon (TOC) and total sulphur (TS)

For elemental analyses, frozen sediment samples were freeze-dried, homogenised in an agate mortar, and placed in capsules until analysis. Biofilm samples were defrosted and placed directly into pre-weighed capsules. The capsules containing the biofilm samples were then weighed after being dried overnight in an oven at 60 °C. Total sulphur (TS) and total organic carbon (TOC) contents were determined using an Elementar Vario Pyro Cube EA CNS.
TOC was measured according to Pella and Colombo (1973). Subsamples of approximately 10 mg were weighed directly into silver capsules and treated with increasing concentrations of HCl (0.1 N, 0.5 N, and 1 N) to remove the carbonate fraction (Nieuwenhuize et al., 1994).
Sulphanilamide (Elementar) was used to calibrate the instrument, and empty capsules were analysed with the samples to correct for blank values. Quality control of measurements was verified against the certified marine sediment reference material PACS-2 (National Research Council Canada) and was within ±2% of the certified value.

4. PRELIMINARY RESULTS

4.1. Hydrography and CTD profiles from the MEFISTO oceanographic campaigns

4.1.1. Physical composition of the water column (salinity and temperature)

The CTD profiles recorded during the two MEFISTO campaigns around Panarea Island, showing salinity and temperature over the water column at the various investigated sites, are presented in Fig. 4.1. An increase in salinity (Fig. 4.1, left panel) of about 0.5 units was observed at almost all sites (excluding Hot & Cold 2), which can be attributed to evaporative processes, coupled with reduced precipitation, affecting the Mediterranean Sea during summer. During both campaigns, the water column was well mixed, with minimal evidence of haloclines. The highest salinities were found at Hot & Cold 1 and Bottaro Downstream (38.4) in September 2024, while the lowest salinity was recorded at Bottaro Single (37.7) in March 2024.
The temperature profiles recorded at the different Panarea sites sampled within the MEFISTO project (Fig. 4.1, right panel) also indicate a mixed water column at all analysed sites and the absence of marked thermoclines. A difference of around 10°C in water temperature was observed at all sites between March and September 2024. The highest in-situ temperature was recorded at Zimmari (25.82°C; Sept-24), and the lowest at an intermediate depth (10 m) at Black Point Smoke station (15.55°C, Mar-24).

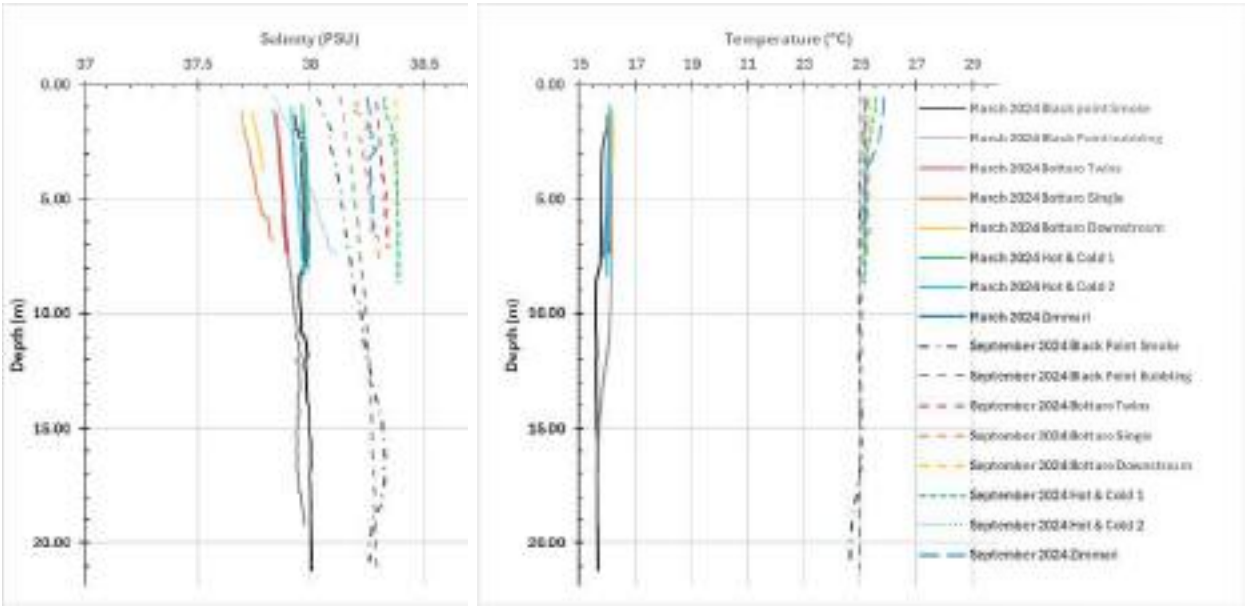

Figure 4.1. CTD profiles for salinity (left panel) and *in-situ* temperature (right panel) recorded during the two Panarea campaigns (March 2024 and September 2024).

The influence of seasonality was much more pronounced in the North Adriatic, as all sites showed strong stratification of the water column in July 2024, whereas homogeneous and mixed conditions were observed in April 2025 (Fig. 4.2). In July 2024, all sites in the Trezze recorded the lowest salinity in the surface water layer (Fig. 4.2, left panel), with a salinity minimum found in BLANK

(31.86 at 1.5 m, Jul-24). Below 10 m depth, salinity became quite homogeneous, with values exceeding 36.6. In April 2025, salinity across all Trezze sites ranged from 37.16 (SAN PIETRO, 1.5 m) to 37.86 (SUDPIASTRA, 16.5 m).
The in-situ temperature measured in the Trezze ranged from a maximum of 28.8 °C (BLANK, 1 m, Jul-24) to a minimum of 12.4 °C, detected at the bottom of all sites in April 2025 (Fig. 4.2, right panel). Under the stratified conditions of July 2024, the temperature decreased from 28 °C at the surface to 19.5 °C at the bottom of SUDPIASTRA.

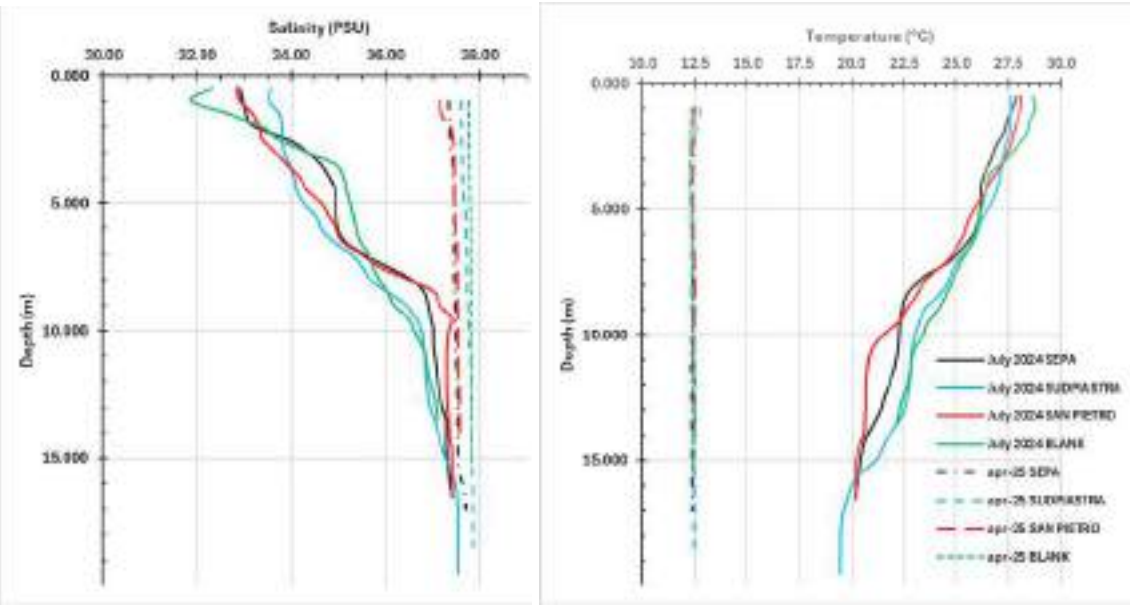

Figure 4.2. CTD profiles for salinity (left panel) and *in-situ* temperature (right panel) recorded during the two Trezze campaigns (July 2024 and April 2025).

4.1.2. pH (nbs) and dissolved oxygen over the water column during MEFISTO campaigns in Panarea and Trezze

Figure 4.2 presents the CTD profiles for pH (left panel) and oxygen saturation (right panel). The pH will be discussed in detail in the Carbonate System parameters section (4.2.1). Briefly, the pH (NBS scale) ranged from 7.31 (Bottaro Twins, 1.2 m, Mar-24) to 8.53 (Black Point Smoke, 0.5 m, Sept-24), with the lowest values observed near the surface at the Bottaro Twins and Single sites, and near the bottom at the Black Point sites. Regarding oxygen saturation, values recorded at the various Panarea sites were all above the saturation point.
In-situ pH and oxygen saturation profiles of the water column during the Trezze campaigns are shown in Fig. 4.4 (left and right panels, respectively). As with the Panarea CTD data, the pH will be discussed in detail in section 4.2.1. Analysis of the CTD profiles shows that pH remained constant throughout the water column in April 2025 (8.27–8.31), while in July 2024 it exhibited a marked decreasing trend with depth (8.41–8.02).
The decreasing pattern in pH was consistent with a drop in oxygen saturation in the deeper layers of the water column at the Trezze sites sampled in July 2024. The lowest level of O_2 saturation was detected at SAN PIETRO (63.09% at 16 m), while the highest saturation was found in the surface

layer of the same site (118.75% at 0.5 m, Jul-24). In April 2025, O_2 saturation ranged between 98% and 99% and remained constant throughout the water column at all assessed sites.

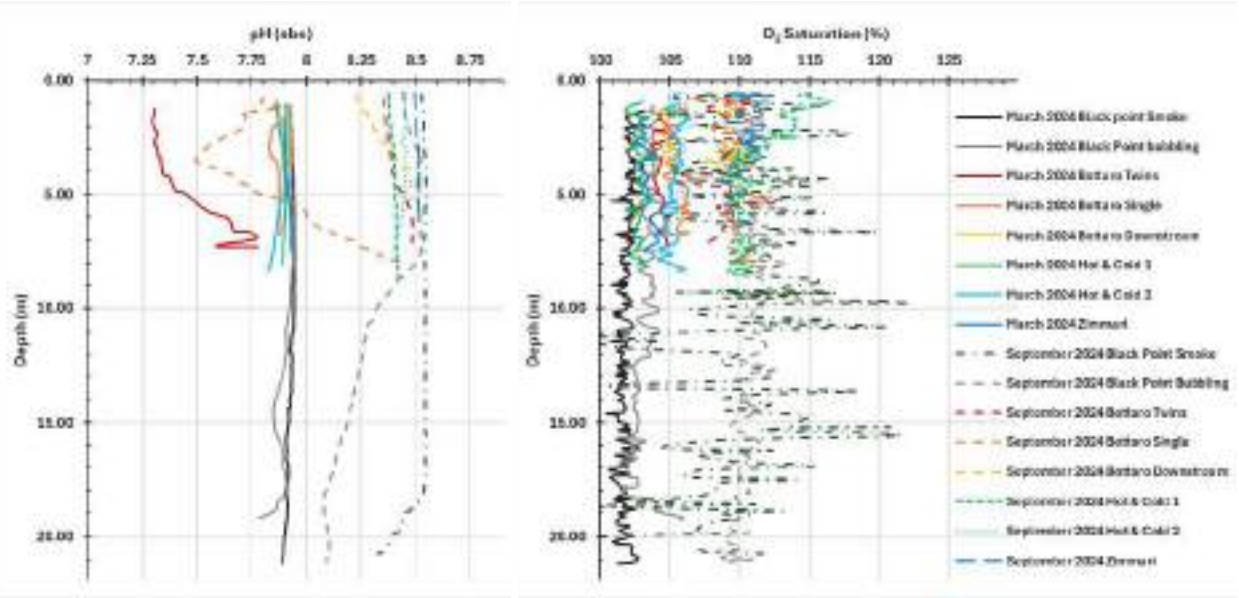

Figure 4.3. CTD profiles for pH (left panel) and O_2 saturation (right panel) recorded during the two Panarea campaigns (March 2024 and September 2024).

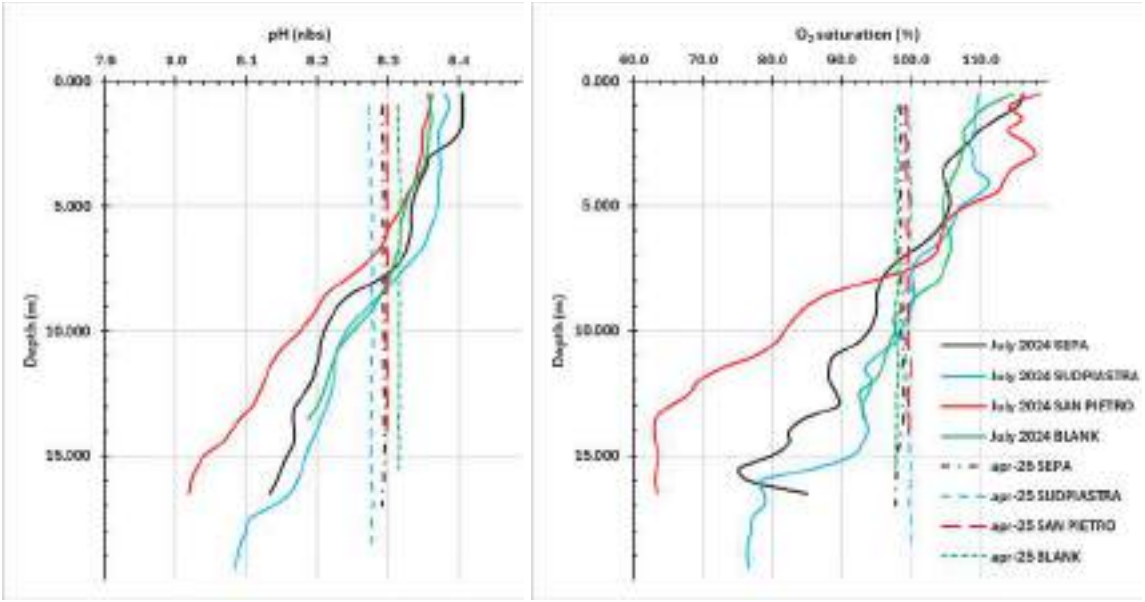

Figure 4.4. CTD profiles for pH (left panel) and O_2 saturation (right panel) recorded during the two Trezze campaigns (July 2024 and April 2025).

4.2. Patterns in the carbonate system over the four MEFISTO Campaigns

4.2.1. Total scale pH referred to the temperature of 25°C (pHT_{25})

The spectrophotometric pH measured at the standard temperature of 25°C (pHT_{25}) during the two MEFISTO campaigns at selected sites in the hydrothermal vent system of Panarea Island ranged from 6.267 (Bottaro Twins SUR Mar-24) to 8.022 (Black Point Smoke SUR Mar-24), with an average value of 7.729 across the area. An overview of the pHT_{25} results is provided in Fig. 4.5. The general pattern observed during the two sampling campaigns indicates higher pHT_{25} values at the surface, with a decreasing trend towards the bottom samples, where the water column is more influenced by hydrothermal emissions. The only two sites that deviate from this pattern are Bottaro Twins and Downstream, a finding possibly related to the intense hydrothermal activity and bubble streams in the area, which may accumulate beneath the seawater–air interface.

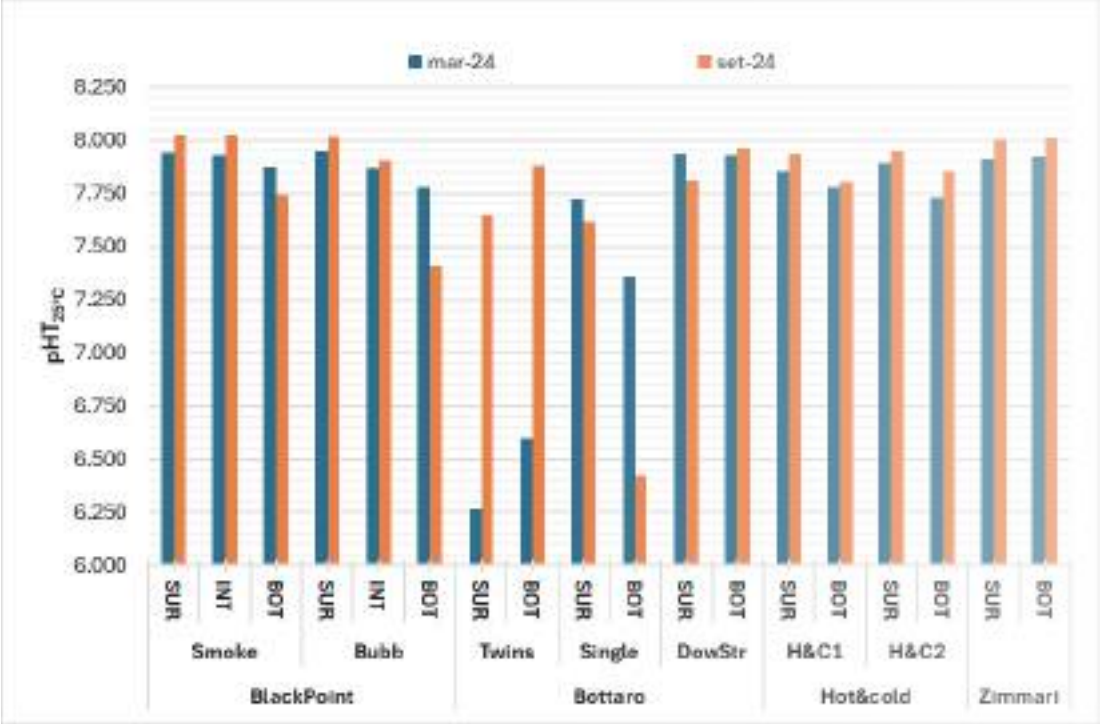

Figure 4.5. Total scale pH referred to the temperature of 25°C (pHT_{25}) recorded during the MEFISTO sampling campaigns in the Panarea island (March 2024 and September 2024).

The pHT_{25} values recorded during the two MEFISTO campaigns (July 2024 and April 2025) at the cold seeps of “trezze” in the North Adriatic are shown in Figure 4.6 and ranged from 7.827 (minimum recorded at SEPA BOT Jul-24) to 8.240 (maximum recorded at SUDPIASTRA SUR Jul-24). The main difference observed between summer (July 2024) and winter (April 2025) conditions is the stratification of the water column. High pHT_{25} values characterised the surface layer at all stations during the July 2024 sampling campaign (pH >8.19), whereas low pHT25 values (<7.90) were observed at all stations except BLANK (BLANK BOT 7.984). Under stratified water column conditions, pH minima are often found in the deeper water layers, as the different

densities of the water masses can act as a cap, reducing gas exchange. This can result in highly oxygenated surface layers, where gas exchange and solar radiation enhance oxygenation through photosynthesis, and hypoxic deeper layers where respiration and remineralisation processes are more pronounced and consume oxygen, resulting in pH minima. This scenario likely occurred during the July 2024 campaign, whereas a homogeneous water column was detected in April 2025, with pHT_{25} >7.92 recorded at all sampled stations.

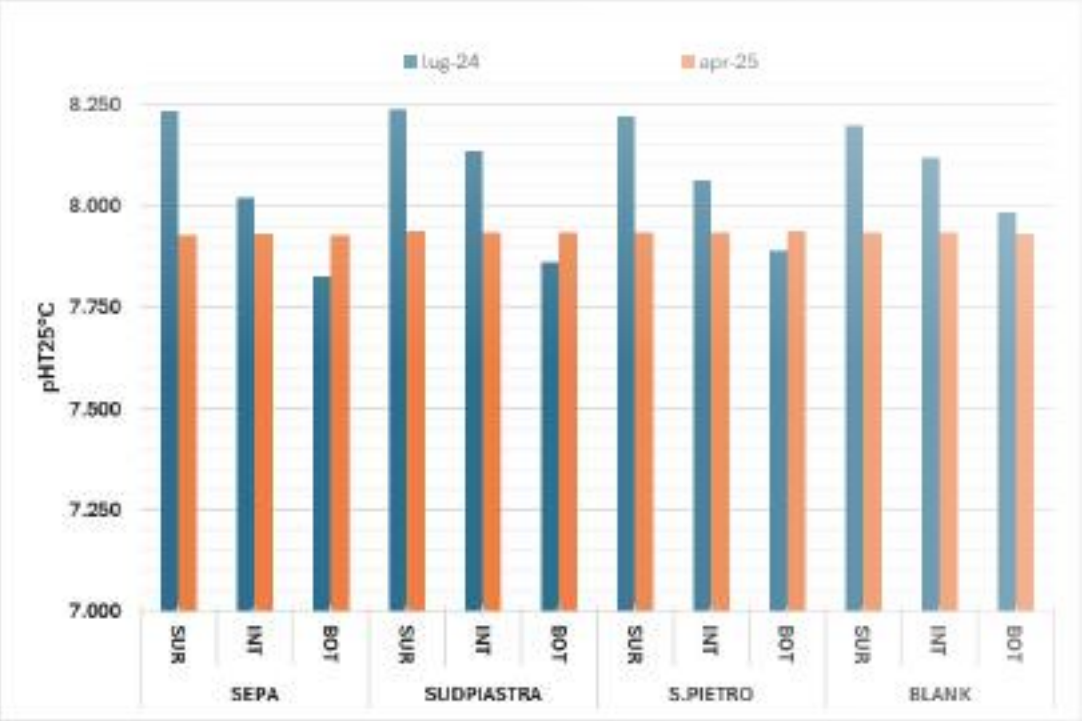

Figure 4.6. Total scale pH referred to the temperature of 25°C (pHT_{25}) recorded during the MEFISTO sampling campaigns in the cold seeps of the Trezze in the North Adriatic (July 2024 and April 2025).

4.2.2. Total alkalinity (TA)

The total alkalinity (TA) recorded during the two MEFISTO campaigns at selected sites in the hydrothermal vent system of Panarea Island ranged from 2328.05 µmol kg^{-1} (Bottaro Single BOT Sept-24) to 2578.95 µmol kg^{-1} (Hot&Cold2 BOT Sept-24), with an average value of 2527.52 µmol kg^{-1} across the area. An overview of the TA results for the different Panarea sites is shown in Fig. 4.7.

Our data indicate a marked seasonal effect on TA, with generally higher TA in September 2024 (end of summer; 2544.74 µmol kg^{-1} ± 0.81, 95% CI, n=18) compared with March 2024 (end of winter; 2510.31 µmol kg^{-1} ± 0.70, 95% CI, n=18). This observation may suggest an effect of evaporation during the warm season in the Mediterranean, as previously reported (Cossarini et al., 2015), and is also supported by the higher salinity recorded in September 2024 (38.24) compared with March 2024 (37.90). Reduced alkalinity was detected in the Bottaro area, specifically at the Bottaro Twins and Single sampling sites.

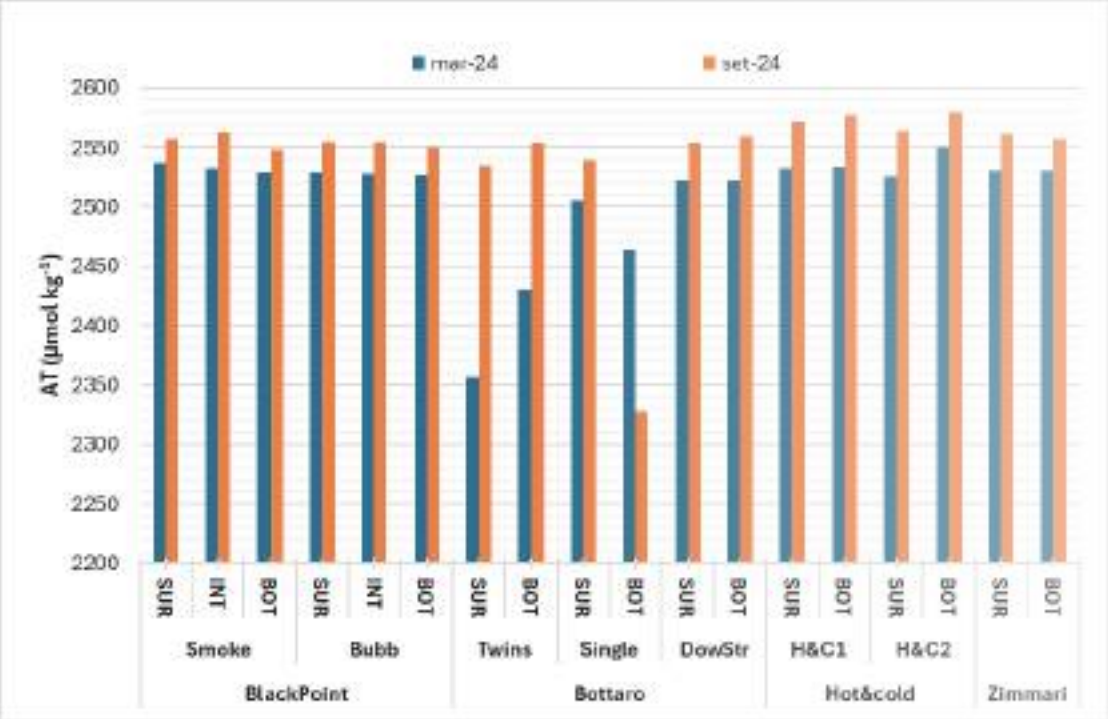

Figure 4.7. Total alkalinity (TA) recorded during the MEFISTO sampling campaigns in the Panarea island (March 2024 and September 2024).

Figure 4.8 shows the patterns in TA detected over the two sampling campaigns conducted in the Trezze (North Adriatic). In the Trezze, TA ranged from 2597.47 µmol kg^{-1} (minimum recorded at SEPA BOT in July 2024) to 2758.53 µmol kg^{-1} (maximum recorded at BLANK SUR in July 2024). The TA recorded during the MEFISTO campaigns at the Trezze indicated different patterns between the two sampling campaigns. Under summer stratified conditions, TA showed a maximum in the surface layer and a minimum in the bottom layer at all stations. In April 2025, with a homogeneous water column, TA content was also highly homogeneous between the sites, with values ranging from 2702.26 to 2643.12 µmol kg^{-1}. The influence of freshwater (salinity <37) was detected in the first 10 m of the water column at all stations during the July 2024 sampling campaign at the Trezze. Rivers flowing into the Gulf of Trieste bring waters very rich in carbonates and CO_2 (Ingrosso et al., 2016; Giani et al., 2023), resulting in a source of TA for the North Adriatic, and possibly explaining the patterns observed in the two MEFISTO campaigns.

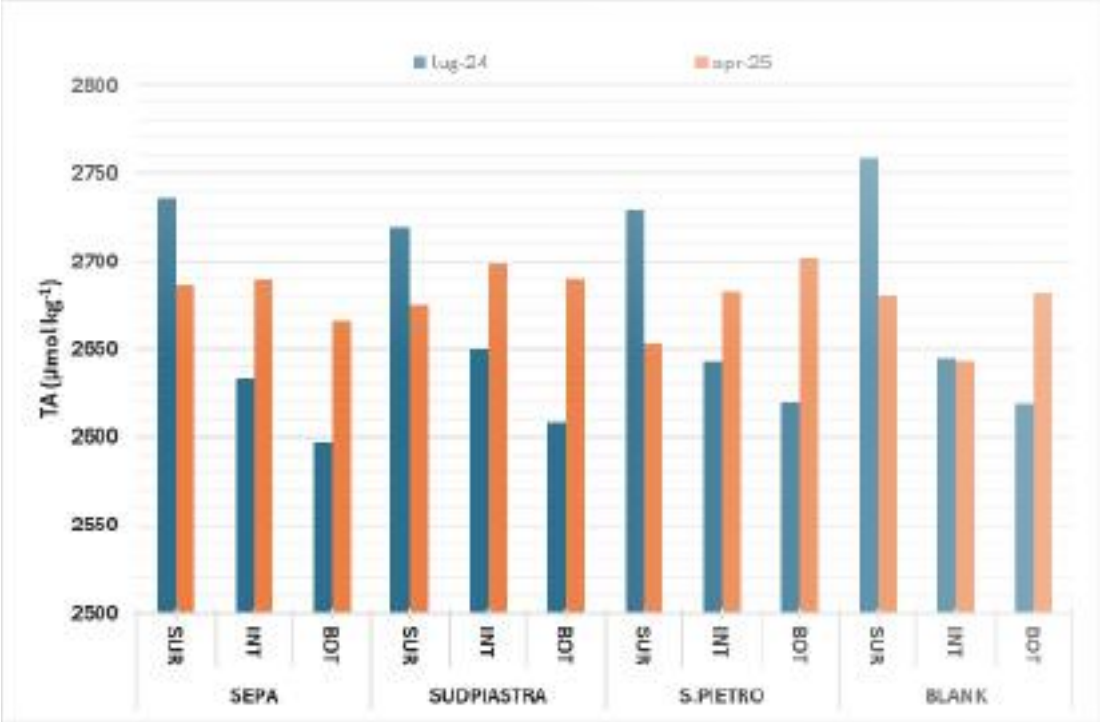

Figure 4.8. Total alkalinity (TA) recorded during the MEFISTO sampling campaigns in the cold seeps of the Trezze in the North Adriatic (July 2024 and April 2025).

4.2.3. Dissolved inorganic Carbon (DIC) and comparison with Total dissolved CO_2 (DIC_{der})

Regarding the instrumental DIC, during the Panarea campaigns, this parameter ranged from a maximum of 2894.23 µmol kg^{-1} (Bottaro Single BOT Sept-24) to a minimum of 2137.68 µmol kg^{-1} (Blackpoint bubbling SUR Mar-24) (Figure 4.9). Generally, higher DIC content was observed during the summer sampling campaign, with the exception of Bottaro Twins SUR Mar-24. These differences can be attributed to seasonality and the higher salinity observed in summer compared to the winter campaign (as discussed for TA).

During the Trezze campaigns, DIC ranged from 2267.41 µmol kg^{-1} (minimum recorded at SUDPIASTRA INT July-24) to 2414.31 µmol kg^{-1} (maximum recorded at SEPA SUR Apr-25, Figure 4.6). As described for TA, water stratification was the main factor influencing DIC during the July 2024 campaign, whereas more homogeneous and higher DIC values were recorded in April 2025, especially when comparing SUP and INT water depths. This pattern is typically observed in the Gulf of Trieste, where DIC tends to decrease in surface and intermediate water layers during the spring and summer period (Cantoni et al., 2012), due to consumption by phytoplankton during photosynthesis, while it accumulates in deeper water layers, where respiration is the dominant biological process.

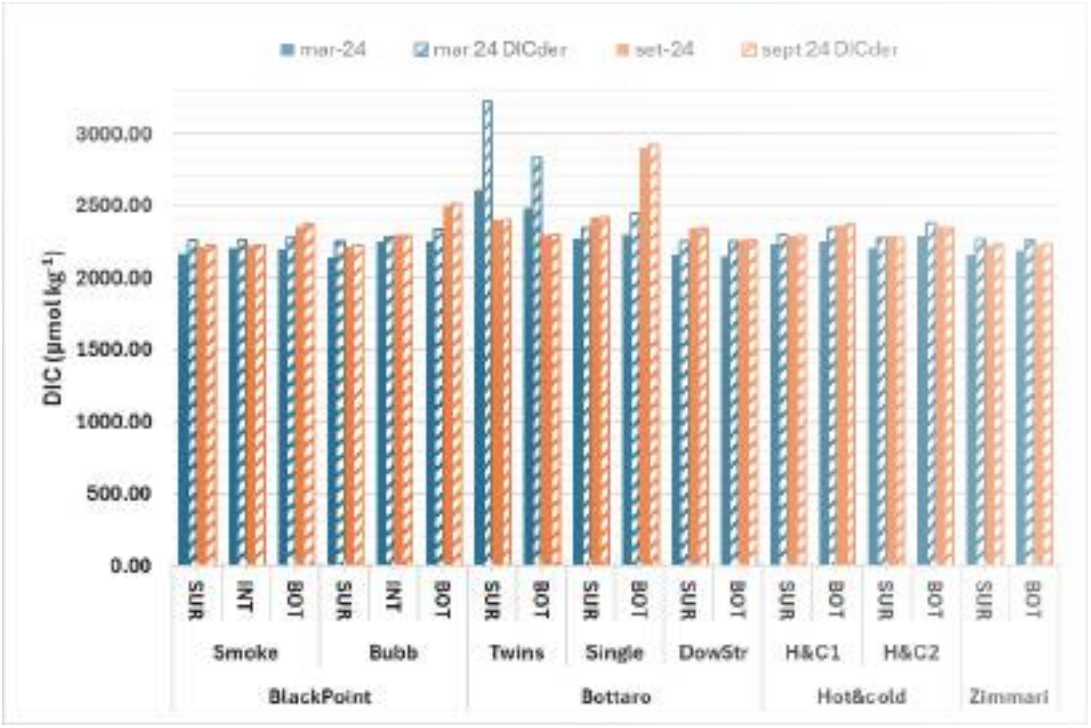

Figure 4.9. Dissolved inorganic Carbon (DIC) and Total Dissolved CO_2 (DIC_{der}) recorded around the Panarea island (March 2024 and September 2024). DIC_{der} was derived from pHT_{insitu} and TA data via CO_2Sys V3.0 software (details in section 3.2.1).

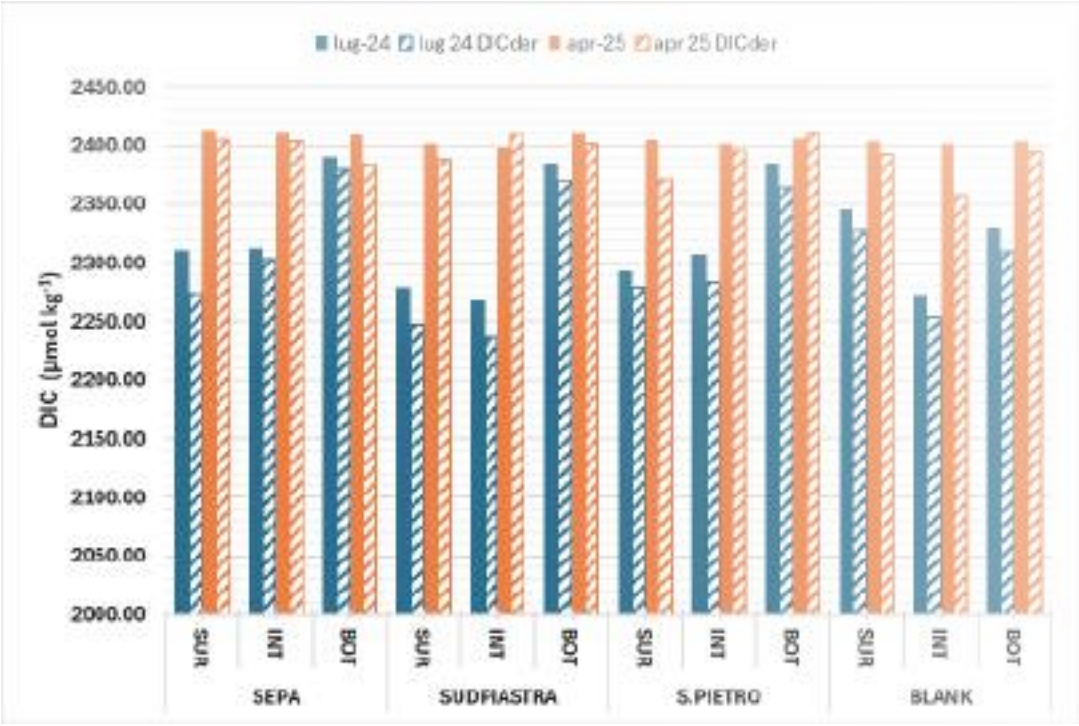

Figure 4.10. Dissolved inorganic Carbon (DIC) and Total Dissolved CO_2 (DIC_{der}) recorded in the cold seeps of the Trezze in the North Adriatic (July 2024 and April 2025). DIC_{der} was derived from pHT_{insitu} and TA data via CO_2Sys V3.0 software (details in section 3.2.1).

In the comparison between instrumental DIC and derived DIC (DIC_{der} – striped bars in Figures 4.9 and 4.10), a certain degree of discrepancy between the two sets of DIC observations can be observed, with the greatest discrepancy found for Bottaro Twins SUR and BOT sampled in March 2024. Several factors may explain these patterns:

- This may be related to the presence of hydrothermal emissions around the island of Panarea, which can alter the water chemistry, causing it to deviate from classical oceanic conditions on which most of the constants and coefficients used for carbonate system derivatisation are based.
- Another possible reason could be the dynamic nature of the hydrothermal system at Panarea, combined with the inevitable time lag between the CTD cast (from which salinity and in situ temperature were obtained) and the closure of the Niskin bottle by divers. This could have led to discrepancies in DICder, as pHT is highly sensitive to temperature.
- Due to the physical characteristics of the rocky and gravelly seabed surrounding Panarea, it was not feasible to deploy the CTD directly at the emission points, whereas Niskin bottles were closed in the proximity of the bubbling sites. This may result in a set of recorded parameters that differ substantially from those at the actual emission point.
- The standard spectrophotometric pH method (SOP 6b) is based on an indicator dye (meta-cresol purple, mCP) with a colour change point between 7.8 and 8.2. Therefore, samples taken very close to the emission point may have pH values well below this range, reducing the sensitivity of the method used.

Considering the previously mentioned points, and the comparison between DIC and DIC_{der} on the Trezze (where, in a less dynamic environment and away from hydrothermal emissions, DIC and IDC_{der} were highly similar), it was decided to use instrumental DIC and TA as carbonate system descriptors, as this pair is also considered the most reliable for calculating the carbonate system under non-standard oceanic conditions (Dickson, 2010).

4.2.4. Derived Carbonate system parameters: partial pressure of CO_2 (pCO_2) and Aragonite saturation state (ΩAra)

The partial pressure of CO_2 (pCO_2), calculated from DIC and TA using CO_2Sys software and recorded during the MEFISTO campaigns around the hydrothermal system of Panarea Island (Figure 4.11), ranged from a minimum of 247.5 µatm (Black Point Bubbling SUR Mar-24) to a maximum of 20,826.1 µatm (Bottaro Single BOT Sept-24). All the highest values were found around the Bottaro site, which was characterised by the highest emissions, mainly composed of CO_2 (see section 4.3.3).

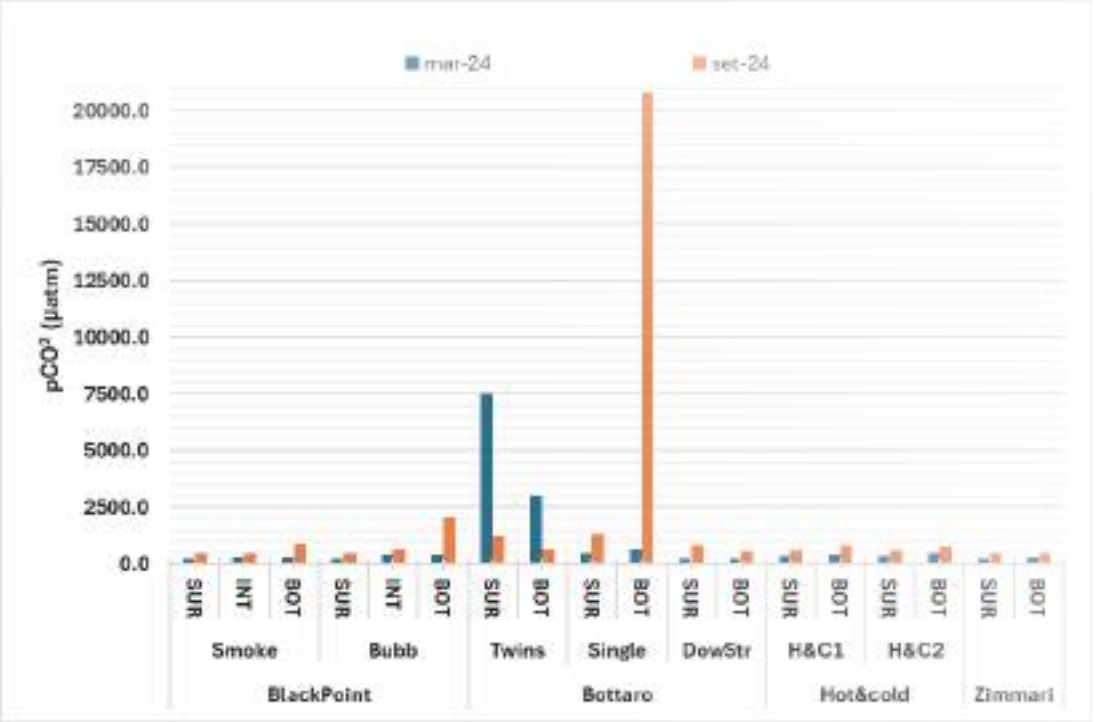

Figure 4.11. partial pressure of CO_2 (pCO_2) recorded around the Panarea island (March 2024 and September 2024). pCO_2 was derived from pHT_{insitu} and TA data via CO_2Sys V3.0 software (details in section 3.2.1).

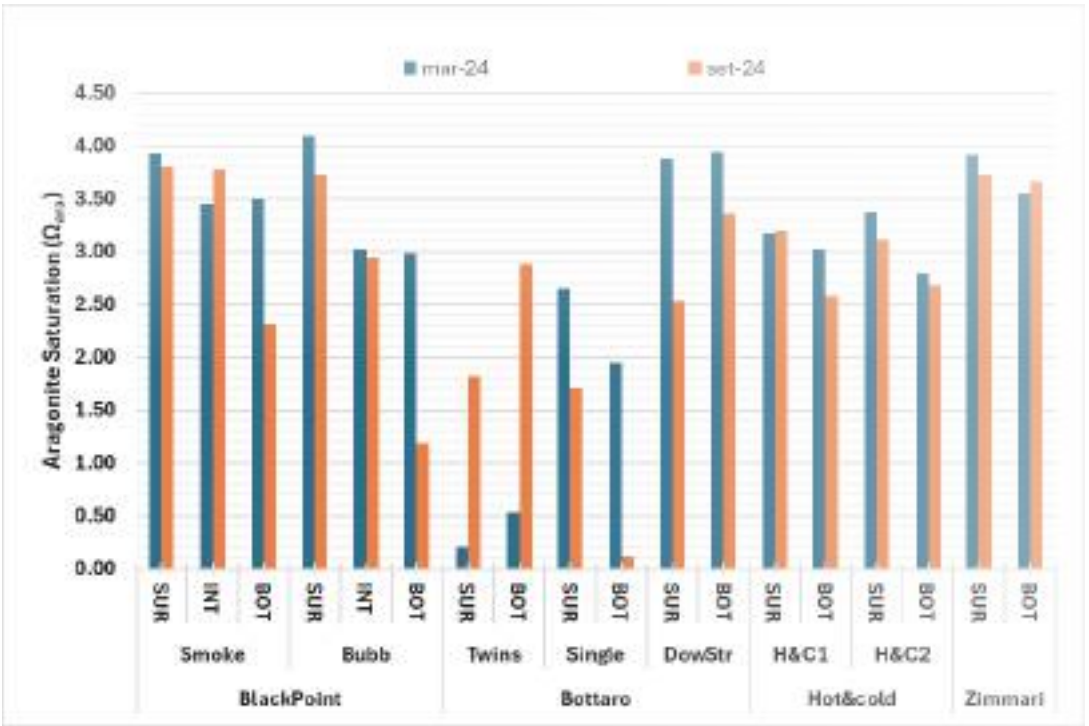

Figure 4.12. Saturation state of aragonite (ΩAra) recorded around the Panarea island (March 2024 and September 2024). ΩAra was derived from pHT_{insitu} and TA data via CO_2Sys V3.0 software (details in section 3.2.1).

As a consequence of the high pCO_2 in the Bottaro areas, these sites also had the lowest aragonite saturation (ΩAra) values, well below the standard oceanic range (2.8–2.9), and in some cases were undersaturated (<1) for this form of calcium carbonate (Figure 4.12). The minimum ΩAra value recorded during the Panarea campaigns was 0.112 (Bottaro Single BOT Sept-24), while the maximum was recorded at Black Point Bubbling SUR Mar-24 (4.09).

The values of pCO_2 and ΩAra recorded during the two Trezze campaigns are shown in Figures 4.13 and 4.14. Both parameters closely followed the patterns previously described for pHT_{25}, TA, and DIC, highlighting the effect of seasonality (summer water stratification versus mixed water column) and displaying an inverse correlation with each other. The pCO2 in Trezze peaked in the deeper layer at all sites sampled in July 2024, with values ranging from 307.1 µatm (minimum at SUDPIASTRA SUR Jul-24) to 671.7 µatm (maximum at SEPA BOT Jul-24).

Conversely, the highest values for ΩAra were recorded in the surface layer of Trezze sites during July 2024, ranging from 2.54 (minimum at SEPA BOT Jul-24) to 5.63 (maximum at SUDPIASTRA SUR Jul-24).

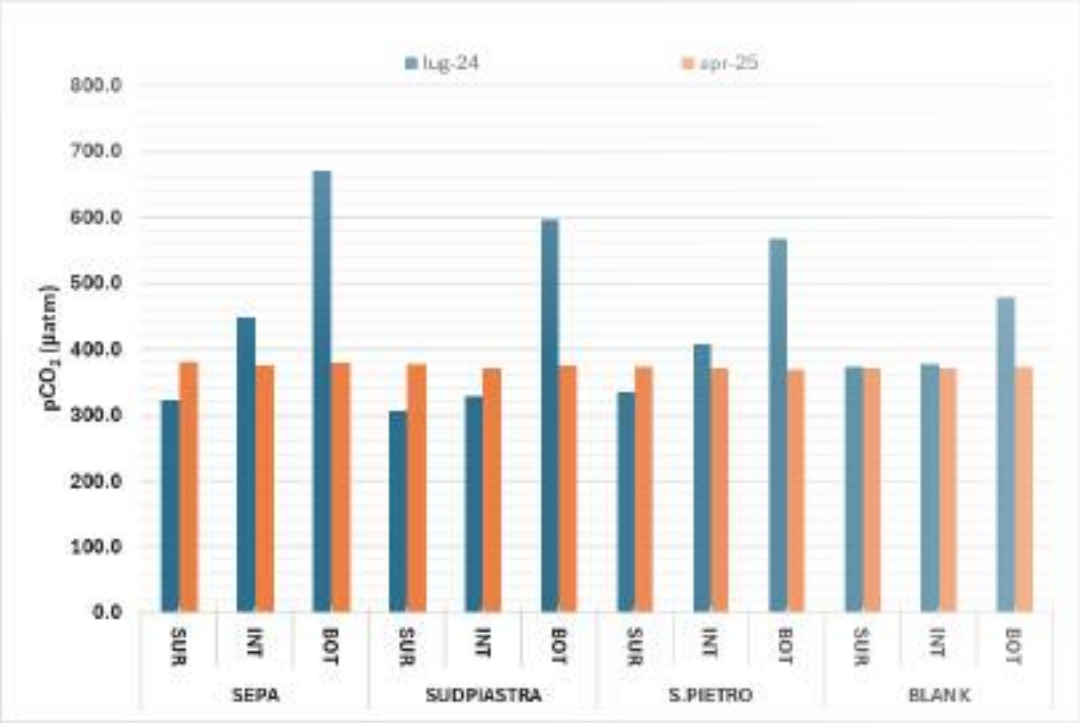

Figure 4.13. Partial pressure of CO_2 (pCO_2) recorded in the cold seeps of the Trezze in the North Adriatic (July 2024 and April 2025). pCO_2 was derived from pHT_{insitu} and TA data via CO_2Sys V3.0 software (details in section 3.2.1).

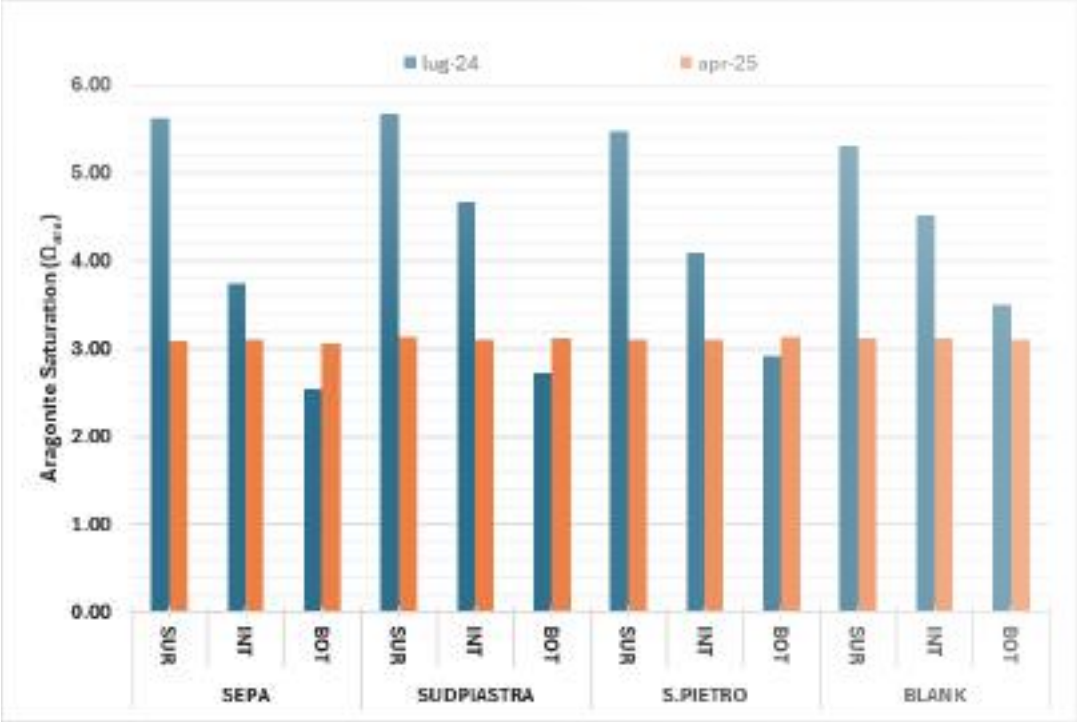

Figure 4.14. Saturation state of aragonite (ΩAra) recorded in the cold seeps of the Trezze in the North Adriatic (July 2024 and April 2025). ΩAra was derived from pHT_{insitu} and TA data via CO_2Sys V3.0 software (details in section 3.2.1).

4.3. Other water chemistry parameters

4.3.1. Inorganic Nutrients (NUT)

Tables 4.1 and 4.2 report the inorganic nutrients (NUT) detected during the four MEFISTO campaigns. Generally nitrites (NO_2^-), nitrates (NO_3^-) and phosphates (PO_4^{3-}) were all in the lower instrumental detection range concentration for all sites monitored around Panarea Island.

Table 4.1 - Inorganic nutrients (NUT) detected during the two MEFISTO campaigns in Panarea. Values within square brackets indicate the September 2024 campaign.

Site	*Depth*	NH_4^+ [µmol L^{-1}]	NO_2^- [µmol L^{-1}]	NO_3^- [µmol L^{-1}]	PO_4^{3-} [µmol L^{-1}]	H_4SiO_4 [µmol L^{-1}]
		Mar-24 (Sept-24)				
Black Point Smoke	SUR	<0.02 (0.20)	<0.01 (0.03	<0.02 (0.09)	<0.01 (0.03)	0.87 (0.59)
	INT	<0.02				0.60)
	BOT	0.0				4.27)
Black Point Bubbling	SUR	<0.0				0.67)
	INT	<0.0				1.15)
	BOT	0.0				1.44)
Bottaro Twins	SUR	0.0				2.90)
	BOT	0.0				0.68)
Bottaro Single	SUR	<0.0				3.94)
	BOT	0.7				5.34)
Bottaro Downstream	SUR	<0.0				1.24)
	BOT	<0.0				1.89)
Hot & Cold1	SUR	0.0				1.81)
	BOT	<0.0				3.26)
Hot & Cold2	SUR	<0.02 (0.06)	0.03 (0.01)	0.02 (0.02)	<0.01 (0.01)	1.79 (2.90)

	BOT	0.04 (0.09)	0.02 (0.01)	0.02 (0.01)	0.01 (<0.01)	9.40 (0.68)
Zimmari	SUR	<0.0				2.27)
	BOT	<0.02 (0.04)	0.01 (0.02)	0.06 (<0.02)	<0.01 (0.02)	1.41 (1.55)

For Panarea campaigns Bottaro area resulted the most rich for ammonia (NH_4^+ Bottaro Single BOT 0.74 and 4.45 µmol L^{-1} respectively for Mar-24 and Sept-24 campaigns) and silicates (H_4SiO_4 Bottaro Single BOT 13.48 and 75.34 µmol L^{-1} respectively for Mar-24 and Sept-24 campaigns).

Table 4.2 - Inorganic nutrients (NUT) detected during the two MEFISTO campaigns in the cold seep system of the Trezze. Values within square brackets indicate the April 2025 campaign.

Site	*Depth*	NH_4^+ [µmol L^{-1}]	NO_2^- [µmol L^{-1}]	NO_3^- [µmol L^{-1}]	PO_4^{3-} [µmol L^{-1}]	H_4SiO_4 [µmol L^{-1}]
		Jul-24 (Apr-25)				
SEPA	SUR	<0.02 (0.07)	0.02 (0.06)	1.05 (1.14)	<0.01 (0.02)	5.14 (3.13)
	INT	<0.0				2.85)
	BOT	1.2				3.79)
SUDPIASTRA	SUR	0.1				3.21)
	INT	<0.0				2.79)
	BOT	0.2				2.53)
SAN PIETRO	SUR	<0.0				3.41)
	INT	<0.0				2.70)
	BOT	2.3				3.14)
BLANK	SUR	<0.0				3.40)
	INT	<0.02 (0.02)	<0.01 (0.03)	0.07 (0.33)	0.02 (0.03)	6.99 (2.71)
	BOT	<0.02 (<0.02)	<0.01 (0.04)	0.06 (0.26)	<0.01 (0.01)	10.93 (2.61)

Concentrations of NO_2^- and PO_4^{3-}, close to the lower instrumental detection limit, were also found during the two campaigns in the Trezze (Table 4.2). The highest content of NH_4^+ was observed in SAN PIETRO BOT during the July campaign (2.35 µmol L^{-1}). For NO_3^-, the mimum content was detected in the intermediate water layer of SEPA during the July sampling (0.05 µmol L^{-1}) whereas the maximum was found in the surface water layer of BLANK in July 2024 (6.24 µmol L^{-1}). Finally, H_4SiO_4 ranged between 1.29 µmol L^{-1}(mimum found in SAN PIETRO INT Jul-24) and 13.88 µmol L^{-1}(maximum found in BLANK SUR Jul-24).

4.3.2. Dissolved Organic Carbon (DOC)

The content of dissolved organic carbon (DOC) recorded during all the MEFISTO oceanografic campaigns is summarised in Table 4.3. Generally the DOC was higher in the cold seep system of the Trezze and had also a seasonal trend with higher values observed during the summer campaigns (July 2024 on the Trezze and September 2024 in Panarea). Aside the 1936.5 µmol L^{-1} detected in the intermediate water layer of Black Point Bubbling in September 2024, value biased by an accidental contamination during the sampling, DOC concentrations in Panarea ranged between the maximum of 94.1 µmol L^{-1} (Black Point Bubbling BOT Sept-24) and the minimum of 59.7 µmol L^{-1} (Black Point Smoke SUR Mar-24).

In the Trezze, the content of DOC varied between 76.6 µmol L^{-1} (minimum found for BLANK BOT Apr-25) and peaked to 163.4 µmol L^{-1}, the maximum detected in SAN PIETRO SUR during the July 2024 campaign.

Table 4.3 - Dissolved organic carbon (DOC) detected during the MEFISTO campaigns in Panarea (March 2024 and September 2024) and in the cold seep system of the Trezze (July 2024 and April 2025). Values within square brackets indicate the September 2024 sampling in Panarea and the April 2025 campaign of the Trezze. In red value biased by an accidental contamination during the sampling.

PANAREA Campaigns		Mar-24 (Sept-24)	**TREZZE Campaigns**		Jul-24 (Apr-25)
Site	Depth	DOC [µmol L^{-1}]	Site	Depth	DOC [µmol L^{-1}]
Black Point Smoke	SUR	59.7 (80.4)	SEPA	SUR	152.7 (78.7)
	INT	60.9 (82.7)		INT	
	BOT			BOT	
Black Point Bubbling	SUR		SUDPIASTRA	SUR	
	INT			INT	
	BOT			BOT	
Bottaro Twins	SUR		SAN PIETRO	SUR	
	BOT			INT	
Bottaro Single	SUR			BOT	
	BOT		BLANK	SUR	
Bottaro Downstream	SUR			INT	
	BOT			BOT	110.8 (76.6)
Hot & Cold1	SUR				
	BOT				
Hot & Cold2	SUR				
	BOT				
Zimmari	SUR	60.9 (84.1)			
	BOT	60.0 (80.2)			

4.3.3. Dissolved gases in the water column

The dissolved gases detected during the MEFISTO campaigns in Panarea are reported in Table 4.4. The highest dissolved CH_4 content was detected in Hot & Cold 1 BOT sampled in Sept-24 (87.05 µatm) whereas the lowest value was found for Black Point Bubbling SUR Sept-24 (1.78 µatm). Traces of CO in Black Point Smoke Mar-24 (7.81 µatm), with all remaining sites showing less or around 1 µatm of such dissolved gas. For what concerns dissolved H_2, the highest content was found for Bottaro Downstream SUR Mar-24 (921.52 µatm), with several sites showing concentrations below the detection limit in the Sept-24 campaign. Dissolved CO_2 was abundant mainly in Bottaro Single BOT Sept-24 (56.23 matm) with the lowest values recorded in Bottaro Bubbling SUR Mar-24 (0.39 matm).

Table 4.4 - Dissolved gases detected during the two MEFISTO campaigns in Panarea. Values within square brackets indicate the September 2024 campaign.

Site	*Depth*	pCH_4 [µatm]	pCO [µatm]	pH_2 [µatm]	pCO_2 [matm]	pO_2+pN_2 [atm]
		Mar-24 (Sept-24)				
Black Point Smoke	SUR	2.05 (6.86)	0.88 (-)	150.02 (42.22)	0.51 (2.81)	0.70 (0.75)
	INT	6.34				(0.56)
	BOT	11.05 (34.41)	0.72 (-)	117.56 (0.00)	0.55 (2.09)	0.74 (0.79)

Black Point Bubbling	SUR	1.78 (6.90)	1.05 (-)	182.81 (63.12)	0.39 (0.77)	0.57 (0.60)
	INT	18.36 (21.44)	1.09 (-)	226.32 (21.00)	0.51 (0.98)	0.71 (0.61)
	BOT	21.69				(0.62)
Bottaro Twins	SUR	3.07				(0.80)
	BOT	2.70				(0.85)
Bottaro Single	SUR	4.51				(0.80)
	BOT	2.83				(0.69)
Bottaro Downstream	SUR	3.20				(0.91)
	BOT	3.33				(0.75)
Hot & Cold1	SUR	27.32				(0.83)
	BOT	48.43				(0.97)
Hot & Cold2	SUR	35.80				(1.04)
	BOT	40.51				(0.80)
Zimmari	SUR	16.96				(0.79)
	BOT	8.77 (16.91)	0.69 (-)	80.64 (0.00)	0.43 (1.06)	0.68 (0.76)

The dissolved gases detected during the MEFISTO campaigns in the cold seep system of the Trezze are reported in Table 4.5. The highest dissolved CH_4 content was detected in SAN PIETRO BOT sampled in Jul-24 (64.93 µatm) whereas the lowest value was found for SEPA INT Apr-25 (5.65 µatm). Traces of CO could be found only in SUDPIASTRA BOT Jul-24 (0.55 µatm) and BLANK BOT Apr-25 (34.59 µatm) with all the remaining sites showing concentrations below detection limit. For what concerns dissolved H_2, this gas peaked in SUDPIASTRA SUR Apr-25 (33.13 matm) and SAN PIETRO INT Jul-24 (16.44 matm), with several sites showing concentrations below the detection limit in both campaigns. Dissolved CO_2 was abundant mainly in SEPA BOT Apr-25 (2.42 matm) with the lowest values being recorded in SAN PIETRO INT Jul-24 (0.42 matm).

Table 4.5 - Dissolved gases detected during the two MEFISTO campaigns in Trezze. Values within square brackets indicate the April 2025 campaign.

Site	*Depth*	pCH_4 [µatm]	pCO [µatm]	pH_2 [µatm]	pCO_2 [matm]	pO_2+pN_2 [atm]
		Jul-24 (Apr-25)				
SEPA	SUR	42.65				(0.83)
	INT	29.91				(0.75)
	BOT	39.64				1.36)
SUDPIASTRA	SUR	13.78				(0.94)
	INT	37.89				(0.78)
	BOT	43.50				(0.99)
SAN PIETRO	SUR	27.35				(0.71)
	INT	35.50				(0.58)
	BOT	64.93				(0.80)
BLANK	SUR	14.97				(0.69)
	INT	17.88				(0.80)
	BOT	57.43 (9.60)	0.00 (34.59)	0.00 (0.00)	0.62 (0.72)	0.70 (0.91)

4.3.4. Gas flux at the air–water interface

Tables 4.6 and 4.7 present the flux of CH_4 and CO_2 measured at the air–water interface during the Panarea and Trezze campaigns. No data are available for the campaign conducted at Trezze in July 2024, and similarly, no measurements of CH_4 were collected by the floating chamber at Panarea in September 2024, as the gas fluxes were probably too low to be detected by the apparatus. It is also likely that at several stations the sea was slightly too rough, preventing the chamber from working properly.

Table 4.6 - Flux of gases detected during the two MEFISTO campaigns in Panarea. Values within square brackets indicate the September 2024 campaign.

Site	CH_4 [g m^{-2} d^{-1}]	CO_2 [g m^{-2} d^{-1}]
	Mar-24 (Sept-24)	
Black Point Smoke	- (-)	10.56 (23.33)
Black Point Bubbling		
Bottaro Twins		
Bottaro Single		
Bottaro Downstream		
Hot & Cold1		
Zimmari	- (-)	- (89.33)

Table 4.7 - Flux of gases detected during the two MEFISTO campaigns in Trezze. Values within square brackets indicate the April 2025 campaign.

Site	CH_4 [g m^{-2} d^{-1}]	CO_2 [g m^{-2} d^{-1}]
	Jul-24 (Apr-25)	
SEPA		
SUDPIASTRA		
SAN PIETRO	- (0.07)	- (-)

4.3.5. Major ions in the water column

Table 4.8 reports all the major ions analysed in the water samples from the sites over Panarea island assessed during the two MEFISTO campaigns (March 2024 and September 2024). NO_3 were also analysed between the main ions but are not reported in table 4.6 or discussed in this paragraph since nitrates have been already considered in section 4.3.1. Over the two campaigns around the hydrothermal system of Panarea island, the major ions detected in the water column ranged between:

- Cations: Li 0.26 - 0.76 meq L^{-1} | Na 439.99 - 563.92 meq L^{-1} | K 9.84 - 12.92 meq L^{-1} | Mg 97.75 - 130.16 meq L^{-1} | Ca 13.80 - 29.81 meq L^{-1}.
- Anions: F 0.04 - 0.18 meq L^{-1} | Cl 538.73 - 655.93 meq L^{-1} | Br 0.99 - 2.49 meq L^{-1} | SO_4 59.50 - 115.11 meq L^{-1} | HCO_3 2.43 - 3.34 meq L^{-1}.

Table 4.9 reports all the major ions analysed in the water samples from the sites over the cold seep system of the Trezze assessed during the two Mefisto campaigns (July 2024 and April 2025). NO3 were also analysed between the main ions but are not reported in table 4.6 or discussed in this paragraph since nitrates have been already considered in section 4.3.1. Over the two campaigns around the cold seeps system of the Trezze, the major ions detected in the water column ranged between:

- Cations: Li 0.25 - 0.26 meq L^{-1} | Na 402.78 - 515.09 meq L^{-1} | K 7.84 - 11.43 meq L^{-1} | Mg 83.07 - 123.41 meq L^{-1} | Ca 19.23 - 26.24 meq L^{-1}.
- Anions: F 0.02 - 0.06 meq L^{-1} | Cl 441.64 - 597.79 meq L^{-1} | Br 0.81 - 1.05 meq L^{-1} | SO_4 48.03 - 60.94 meq L^{-1} | HCO_3 2.47 - 3.24 meq L^{-1}.

Table 4.8 - Major Ions detected in the water column during the two MEFISTO campaigns in Panarea. Values within square brackets indicate the September 2024 campaign.

Major Ions detected in Panarea Campaigns - Water column - Cations [meq L^{-1}] - Mar-24 (Sept-24)						
Site	Depth	Li	Na	K	Mg	Ca
Black Point Smoke	SUR	0.70 (-)	483.27 (523.18)	12.92 (12.57)	110.50 (128.81)	29.81 (24.49)
	INT	0.72 (-)	488.07 (497.22)	13.37 (10.87)	113.83 (107.01)	14.53 (23.15)
	BOT	0.72				4.82)
Black Point Bubbling	SUR	0.26				3.64)
	INT	0.76				2.95)
	BOT	0.70				2.76)
Bottaro Twins	SUR	0.70				3.49)
	BOT	0.72				4.85)
Bottaro Single	SUR	0.70				3.67)
	BOT	0.70				6.77)
Bottaro Downstream	SUR	0.70				3.55)
	BOT	0.70				5.10)
Hot & Cold1	SUR	0.26				4.74)
	BOT	0.26				3.07)
Hot & Cold2	SUR	0.70 (-)	480.75 (501.28)	12.76 (10.84)	108.27 (106.78)	28.31 (22.98)
	BOT	0.26 (-)	495.80 (527.52)	9.82 (11.44)	109.81 (112.37)	21.82 (23.92)

Zimmari	SUR	0.70 (-)	479.87 (534.04)	12.86 (13.35)	111.13 (126.99)	23.13 (23.03)
	BOT	0.70 (-)	489.20 (563.52)	12.70 (13.55)	108.05 (112.37)	20.25 (23.89)
Major Ions detected in Panarea Campaigns - Water column - Anions [meq L^{-1}] - Mar-24 (Sept-24)						
Site	Depth	F	Cl	Br	SO_4	HCO_3
Black Point Smoke	SUR	0.18 (-)	558.61 (645.82)	1.02 (1.47)	61.32 (66.04)	2.66 (2.60)
	INT	0.18 (-)	547.43 (606.56)	1.03 (1.36)	59.52 (60.80)	2.91 (2.84)
	BOT	0.1				(2.55)
Black Point Bubbling	SUR	0.1				(2.57)
	INT	0.1				(2.69)
	BOT	0.1				(2.60)
Bottaro Twins	SUR	0.1				(2.45)
	BOT	0.1				(3.34)
Bottaro Single	SUR	0.1				(2.52)
	BOT	0.0				(2.28)
Bottaro Downstream	SUR	0.1				(2.58)
	BOT	0.0				64)
Hot & Cold1	SUR	0.0				(2.92)
	BOT	0.0				(2.62)
Hot & Cold2	SUR	0.1				(2.82)
	BOT	0.0				(2.55)
Zimmari	SUR	0.11 (-)	550.12 (630.37)	1.04 (0.99)	60.84 (66.16)	2.78 (2.61)
	BOT	0.10 (-)	583.21 (606.32)	1.04 (1.36)	60.21 (115.11)	2.72 (2.87)

Table 4.9 - Major Ions detected in the water column during the two MEFISTO campaigns in the Trezze. Values within square brackets indicate the April 2025 campaign.

Major Ions detected in Trezze Campaigns - Water column - Cations [meq L^{-1}] - Jul-24 (Apr-25)						
Site	Depth	Li	Na	K	Mg	Ca
SEPA	SUR	0.25 (-)	412.43 (505.52)	7.84 (11.38)	92.92 (114.64)	19.94 (23.66)
	INT	0				23.00)
	BOT	0				22.49)
SUDPIASTRA	SUR	0				22.96)
	INT	0				21.10)
	BOT	0				22.96)
SAN PIETRO	SUR					22.25)
	INT	0				22.70)
	BOT	0				22.73)
BLANK	SUR	0				24.04)
	INT					23.50)
	BOT	0.26 (-)	464.97 (509.69)	9.29 (11.23)	105.41 (115.49)	20.73 (23.23)
Major Ions detected in Trezze Campaigns - Water column - Anions [meq L^{-1}] - Jul-24 (Apr-25)						
Site	Depth	F	Cl	Br	SO_4	HCO_3
SEPA	SUR	0.05 (-)	441.64 (586.79)	0.86 (0.82)	49.22 (53.95)	3.24 (2.64)
	INT	0.06 (-)	519.61 (568.30)	1.00 (0.87)	58.90 (53.79)	3.02 (2.83)
	BOT					(2.63)
SUDPIASTRA	SUR					(2.69)
	INT					(2.47)
	BOT					(2.51)
SAN PIETRO	SUR					(2.49)
	INT					(2.64)
	BOT	0.06 (-)	536.69 (577.58)	1.02 (0.87)	60.93 (55.11)	2.70 (2.75)

BLANK	SUR	0.04 (-)	428.19 (582.67)	0.83 (0.87)	48.03 (54.62)	2.81 (2.72)
	SUR	0.0				8)
	BOT	0.00 (-)	330.33 (370.83)	1.02 (0.85)	66.82 (53.81)	2.77 (2.57)

4.3.6. Trace elements in the water column

Table 4.10 shows a selection of trace elements detected over the two MEFISTO campaigns completed on different sites of the hydrothermal system of Panarea island; Aluminium (Al), Berillio (Be), Cadmium (Cd), Cobalt (Co), Chromium (Cr), Nikel (Ni), Selenium (Se), Titanium (Ti), Thallium (Tl) and Zinc (Zn) were also analysed for all samples, but are not listed in Tab 4.10 due to their low concentration closer or below the limit of detection of the instrumentation used for the analysis. The trace elements detected in the water samples collected during the two campaigns over Panarea island ranged as follow:

As 1.74 - 2.62 µg L^{-1} | B 6.53 - 7.97 mg L^{-1} | Ba 11.74 - 16.65 µg L^{-1} | Br 0.12 - 0.15 g L^{-1} | Cs 0.48 - 1.50 µg L^{-1} | Cu <7 - 88.80 µg L^{-1} | Fe <0.6 - 26.2 µg L^{-1} | Li 0.18 - 0.26 mg L^{-1} | Mn 1.54 - 67.10 µg L^{-1} | Mo 4.99 - 16.55 µg L^{-1} | Pb <0.1 - 0.90 µg L^{-1} | Rb 0.18 - 0.23 mg L^{-1} | Sb <0.1 - 0.55 µg L^{-1} | Si 5.39 - 6.09 mg L^{-1} | Sr 12.10 - 14.61 mg L^{-1} | U 3.65 - 4.81 µg L^{-1} | V 2.62 - 4.81 µg L^{-1}.

Table 4.10 - List of trace elements detected in the water column during the two MEFISTO campaigns in the hydrothermal system surrounding Panarea island.

	Trace Elements water column Panarea Mar-24										
Site	As [µg L^{-1}]	B [mg L^{-1}]	Ba [µg L^{-1}]	Br [g L^{-1}]	Cs [µg L^{-1}]	Cu [µg L^{-1}]	Fe [µg L^{-1}]	Li [mg L^{-1}]	Mn [µg L^{-1}]	Mo [µg L^{-1}]	Pb [µg L^{-1}]
Black Point Bubbling	2.39	7.97	14.11	0.14	0.97	<7	26.2	0.22	11.2	16.55	0.47
Bottaro Twins	2.05										<0.1
Bottaro Single	2.47										<0.1
Bottaro Downstream	2.32										<0.1
Hot & Cold1	1.74										<0.1
Zimmari	2.62	7.93	16.65	0.15	1.11	58.60	15.10	0.26	5.78	15.59	0.90
Site	Rb [mg L^{-1}]	Sb [µg L^{-1}]	Si [mg L^{-1}]	Sr [mg L^{-1}]	U [µg L^{-1}]	V [µg L^{-1}]					
Black Point Bubbling	0.21	0.55	5.66	13.87	4.15	3.54					
Bottaro Twins	0.2					07					
Bottaro Single	0.2					56					
Bottaro Downstream	0.2					65					
Hot & Cold1	0.1					62					
Zimmari	0.23	0.29	5.85	14.61	4.81	4.81					

Table 4.11 shows a selection of trace elements detected over the two MEFISTO campaigns completed on different sites of the cold seep system of the Trezze in the North Adriatic; Al, Be, Co, Copper (Cu), Iron (Fe), Se, Ti, Tl and Zn were also analysed for all samples, but are not listed in Tab 4.11 due to their low concentration closer or below the limit of detection of the instrumentation used for the analysis. The trace elements detected in the water samples collected during the two campaigns over Trezze ranged as follow:

As 1.58 - 2.62 µg L^{-1} | B 6.71 - 7.49 mg L^{-1} | Ba 7.97 - 18.05 µg L^{-1} | Br 0.10 - 0.17 g L^{-1} | Cd <0.3 - 0.82 µg L^{-1} | Cr <0.5 - 1.79 µg L^{-1} | Cs 0.43 - 1.79 µg L^{-1} | Li 0.19 - 0.40 mg L^{-1} | Mn 0.63 - 34.36 µg L^{-1} | Mo 13.38 - 22.20 µg L^{-1} | Ni <0.5 - 2.39 µg L^{-1} | Pb <0.3 - 1.48 µg L^{-1} | Rb 0.15 - 0.27 mg L^{-1} | Sb <0.5 - 0.1.51 µg L^{-1} | Si <0.5 - 1.85 mg L^{-1} | Sr 10.35 - 17.04 mg L^{-1} | U 3.30 - 6.24 µg L^{-1} | V 2.10 - 3.90 µg L^{-1}.

Table 4.11 - List of trace elements detected in the water column during the two MEFISTO campaigns in the cold seep system of the Trezze. Values between brackets refer to the April 2025 sampling campaign.

	Trace elements water column Trezze - Jul-24 (Apr-25)										
Site	As [µg L^{-1}]	B [mg L^{-1}]	Ba [µg L^{-1}]	Br [g L^{-1}]	Cd [µg L^{-1}]	Cr [µg L^{-1}]	Cs [µg L^{-1}]	Li [mg L^{-1}]	Mn [µg L^{-1}]	Mo [µg L^{-1}]	Ni [µg L^{-1}]
SEPA	2.62 (2.03)										0.24 (<0.5)
SUDPIASTRA	2.49 (2.17)										2.39 (<0.5)
SAN PIETRO	2.75 (1.58)										0.86 (<0.5)
BLANK	2.71 (1.64)	(4.53)	(9.79)	(0.11)	(0.54)	(<0.5)	(0.43)	(0.19)	(0.63)	(14.00)	0.27 (<0.5)
Site	Pb [µg L^{-1}]	Rb [mg L^{-1}]	Sb [µg L^{-1}]	Si [mg L^{-1}]	Sr [mg L^{-1}]	U [µg L^{-1}]	V [µg L^{-1}]				
SEPA	0.59 (0.7	0.19	<0.5	0.63	12.82	3.97	3.90 .79)				
SUDPIASTRA	0.6 (0.4						.10 .70)				
SAN PIETRO	0.1 (1.4						.99 .10)				
BLANK	<0. (0.42)	(0.17)	(<0.5)	(1.15)	(10.78)	(3.30)	.33 (2.30)				

4.4. Interstitial fluids composition

4.4.1 Major Ions

Table 4.12 reports all the major ions analysed in the fluids samples from the sites over Panarea island assessed during the two Mefisto campaigns (March 2024 and September 2024). Over the two campaigns around the hydrothermal system of Panarea island, the major ions detected in the interstitial fluids ranged between:

- Interstitial fluids:
  - Cations: Li 0.70 - 0.76 meq L^{-1} | Na 474.22 - 534.55 meq L^{-1} | K 10.44 - 15.34 meq L^{-1} | Mg 107.04 - 130.48 meq L^{-1} | Ca 18.22 - 26.88 meq L^{-1}.
  - Anions: F 0.07 - 0.20 meq L^{-1} | Cl 526.85 - 656.12 meq L^{-1} | Br 1.03 - 1.61 meq L^{-1} | SO_4 59.50 - 67.04 meq L^{-1} | HCO_3 1.31 - 2.84 meq L^{-1}.
- Hydrothermal fluids:
  - Cations: Li 0.26 - 1.74 meq L^{-1} | Na 474.82 - 544.23 meq L^{-1} | K 10.34 - 36.18 meq L^{-1} | Mg 58.39 - 128.99 meq L^{-1} | Ca 23.32 - 175.6 meq L^{-1}.
  - Anions: F 0.03 - 0.86 meq L^{-1} | Cl 547.14 - 783.32 meq L^{-1} | Br 1.02 - 1.33 meq L^{-1} | SO_4 18.34 - 64.97 meq L^{-1} | HCO_3 0.84 - 2.74 meq L^{-1}.

Table 4.12 - Major Ions detected in the fluids (IS: Interstitial fluid; HT hydrothermal fluid) during the two MEFISTO campaigns over the hydrothermal system of Panarea. Values within square brackets indicate the September 2024 campaign.

Major Ions detected in Panarea Campaigns - Interstitial/hydrothermal fluids - Cations [meq L^{-1}] - Mar-24 (Sept-24)						
Site	Fluid	Li	Na	K	Mg	Ca
Black Point Smoke	IS	- (-)	- (534.55)	- (15.34)	- (120.02)	- (18.22)
	HT	1.74 (1.19)	474.82 (511.58)	36.18 (34.31)	58.39 (73.14)	175.6 (167.66)
Bottaro Twins	IS	[illegible]				[illegible]7)
Bottaro Single	IS	0.7[illegible]				[illegible].70)
	HT	0.40				[illegible].93)
Bottaro Downstream	IS	[illegible]				[illegible].04)
Hot & Cold1	IS	0.7[illegible]				[illegible].82)
	HT	0.7[illegible]				[illegible].70)
Hot & Cold2	IS	0.7[illegible]				[illegible].59)
	HT	0.70 (-)	514.33 (509.56)	12.83 (12.59)	110.21 (123.89)	29.58 (24.11)
Major Ions detected in Panarea Campaigns - Interstitial/hydrothermal fluids - Anions [meq L^{-1}] - Mar-24 (Sept-24)						
Site	Depth	F	Cl	Br	SO_4	HCO_3
Black Point Smoke	IS	- (-)	- (656.12)	- (-)	- (67.04)	- (2.23)
	HT	0.2[illegible]				[illegible]
Bottaro Twins	IS	[illegible]				[illegible]3)
Bottaro Single	IS	0[illegible]				[illegible].76)
	HT	0[illegible]				[illegible]4)
Bottaro Downstream	IS	0[illegible]				[illegible].15)
Hot & Cold1	IS	0[illegible]				[illegible].11)
	HT	0.03 (-)	547.14 (633.30)	1.03 (-)	61.55 (64.97)	- (2.74)

Hot & Cold2	IS	0.0				50)
	HT	0.1 (-)				(-)

Table 4.13 reports all the major ions analysed in the fluids samples from the sites of the cold seeps system of the Trezze assessed during the two Mefisto campaigns (July 2024 and April 2025). Major ions in the Trezze interstitial fluids ranged between:

- Interstitial fluids:
  - Cations: Li 0.26 meq L^{-1} | Na 445.09 - 522.95 meq L^{-1} | K 9.35 - 12.47 meq L^{-1} | Mg 101.12 - 118.45 meq L^{-1} | Ca 21.50 - 24.01 meq L^{-1}.
  - Anions: F 0.05 - 0.06 meq L^{-1} | Cl 525.68 - 591.49 meq L^{-1} | Br 0.84 - 1.02 meq L^{-1} | SO_4 51.22 - 59.86 meq L^{-1} | HCO_3 2.62 - 2.90 meq L^{-1}.

Table 4.13 - Major Ions detected in the interstitial fluids (IS) during the two MEFISTO campaigns in the cold seeps system of the Trezze. Values within square brackets indicate the April 2025 campaign.

		Major Ions Interstitial fluids Trezze - Cations [meq L^{-1}] - Jul-24 (Apr-25)				
Site	Fluid	Li	Na	K	Mg	Ca
SEPA	IS	0.26 (-)	522.95 (445.09)	11.64 (12.47)	118.45 (101.12)	23.15 (21.50)
SUDPIASTRA	IS	0.2				87)
SAN PIETRO	IS	0.26 (-)	473.70 (507.17)	10.31 (11.15)	104.91 (115.22)	21.58 (24.01)
		Major Ions Interstitial fluids Trezze - Anions [meq L^{-1}] - Jul-24 (Apr-25)				
Site	Fluid	F	Cl	Br	SO_4	HCO_3
SEPA	IS	0.05 (-)	525.68 (591.49)	1.02 (0.84)	59.52 (51.22)	2.77 (2.62)
SUDPIASTRA	IS	0.0				58)
SAN PIETRO	IS	0.06 (-)	528.09 (585.07)	1.02 (0.86)	59.71 (55.71)	2.90 (2.55)

4.4.2. Trace Elements

Table 4.14 shows a selection of trace elements detected in the fluids (interstitial and hydrothermal) over the two MEFISTO campaigns completed on different sites of the hydrothermal system of Panarea island; Al, Be, Cd, Se and Ti were also analysed for all samples, but are not listed in Tab 4.14 due to their low concentration closer or below the limit of detection of the instrumentation used for the analysis.

The trace elements detected in the interstitial fluids collected during the two campaigns over Panarea island ranged as follow:

As 1.53 - 15.6 µg L^{-1} | B 6.53 - 8.14 mg L^{-1} | Ba 12.25 - 128.6 µg L^{-1} | Br 0.12 - 0.14 g L^{-1} | Co <0.1 - 0.62 µg L^{-1} | Cr <0.7 - 3.14 µg L^{-1} | Cs 0.48 - 16.18 µg L^{-1} | Cu <0.01 - 0.37 mg L^{-1} | Fe <0.6 - 15254 µg L^{-1} | Li 0.18 - 0.42 mg L^{-1} | Mn <0.01 - 3.76 mg L^{-1} | Mo 0.8 - 27.41 µg L^{-1} | Ni <0.8 - 1.97 µg L^{-1} | Pb <0.1 - 25.24 µg L^{-1} | Rb 0.20 - 0.33 mg L^{-1} | Sb <0.1 - 0.27 µg L^{-1} | Si 3.79 - 126.20 mg L^{-1} | Sr

11.73 - 14.24 mg L^{-1} | Tl <0.05 - 0.60 µg L^{-1} | U 1.03 - 5.46 µg L^{-1} | V 0.92 - 8.25 µg L^{-1} | Zn <3 - 36.3 µg L^{-1}.

The trace elements detected in the hydrothermal fluids collected during the two campaigns over Panarea island ranged as follow:

As 2.26 - 383.0 µg L^{-1} | B 6.19 - 102.86 mg L^{-1} | Ba 14.94 - 1106 µg L^{-1} | Br 0.11 - 0.16 g L^{-1} | Co <0.1 - 1.12 µg L^{-1} | Cr <0.7 - 2.81 µg L^{-1} | Cs 1.09 - 2765 µg L^{-1} | Cu 0.01 - 0.34 mg L^{-1} | Fe <0.6 - 20520 µg L^{-1} | Li 0.20 - 42.28 mg L^{-1} | Mn 0.08 - 294.99 mg L^{-1} | Mo 0.67 - 19.16 µg L^{-1} | Ni <0.8 - 1.97 µg L^{-1} | Pb 0.25 - 61.79 µg L^{-1} | Rb 0.17 - 10.89 mg L^{-1} | Sb <0.1 - 0.34 µg L^{-1} | Si 4.15 - 151.60 mg L^{-1} | Sr 10.63 - 104.88 mg L^{-1} | Tl 0.12 - 130.00 µg L^{-1} | U 1.28 - 5.03 µg L^{-1} | V 1.65 - 115.1 µg L^{-1} | Zn <3 - 58554 µg L^{-1}.

Table 4.15 shows a selection of trace elements detected over the two MEFISTO campaigns completed on different sites of the cold seep system of the Trezze in the North Adriatic; Al, Be, Co, Cu, Se, Ti, Tl and Zn were also analysed for all samples, but are not listed in Tab 4.15 due to their low concentration closer or below the limit of detection of the instrumentation used for the analysis. The trace elements detected in the interstitial fluid samples collected during the two campaigns over Trezze ranged as follow:

As 1.71 - 5.83 µg L^{-1} | B 5.12 - 9.26 mg L^{-1} | Ba 10.32 - 24.40 µg L^{-1} | Br 0.11 - 0.21 g L^{-1} | Cd 0.35 - 0.80 µg L^{-1} | Cr <0.5 - 2.30 µg L^{-1} | Cs 0.56 - 1.19 µg L^{-1} | Fe <2 - 65.60 µg L^{-1} | Li 0.24 - 0.65 mg L^{-1} | Mn 8.58 - 117.56 µg L^{-1} | Mo 4.638 - 20.30 µg L^{-1} | Ni <0.5 - 2.10 µg L^{-1} | Pb <0.3 - 7.72 µg L^{-1} | Rb 0.17 - 0.33 mg L^{-1} | Sb 0.28 - 5.43 µg L^{-1} | Si 0.54 - 1.78 mg L^{-1} | Sn <1 - 3.52 µg L^{-1} | Sr 11.90 - 21.46 mg L^{-1} | U 3.56 - 8.89 µg L^{-1} | V 6.12 - 13.11 µg L^{-1}.

Table 4.14 - List of trace elements detected in the interstitial (IS) and hydrothermal (HT) fluids during the two MEFISTO campaigns in the hydrothermal system surrounding Panarea island. BlPt Smoke - BlackPoint Smoke; Bott Sing - Bottaro Single; Bott DwSt - Bottaro Downstream; H&C1 - Hot & Cold 1; H&C2 - Hot & Cold 2. Values between brackets refer to the September 2024 sampling campaign.

		Trace elements Fluids Panarea Mar-24 (Sept-24)										
Site	*Fluid*	As [µg L^{-1}]	B [mg L^{-1}]	Ba [µg L^{-1}]	Br [g L^{-1}]	Co [µg L^{-1}]	Cr [µg L^{-1}]	Cs [µg L^{-1}]	Cu [mg L^{-1}]	Fe [µg L^{-1}]	Li [mg L^{-1}]	Mn [mg L^{-1}]
BlPt Smoke	IS	2.1 (15.6)	7.67 (8.06)	12.25 (29.39)	0.13 (0.13)	<0.1 (0.45)	0.71 (2.28)	0.98 (2.36)	0.12 (0.36)	7.75 (1875)	0.25 (0.42)	0.01 (0.83)
	HT	11.1 (383.0)										0.08 (294.99)
Bott Sing	IS	5.37 (1.4)										0.05 (0.27)
	HT	3.58 (7.86)										0.82 (42.28)
Bott DwSt	IS	2.32 (-)										<0.01 (-)
H&C1	IS	2.96 (7.97)										0.10 (3.76)
	HT	5.13 (2.26)										3.66 (0.16)
H&C2	IS	1.53 (3.34)										0.05 (0.04)
	HT	5.14 (15.6)	7.26 (8.52)	104.5 (141)	0.13 (0.14)	1.12 (0.13)	<0.7 (<0.7)	14.88 (17.18)	0.34 (0.17)	14363 (20520)	0.24 (0.29)	4.13 (4.44)
Site	Fluid	Mo [µg L^{-1}]	Ni [µg L^{-1}]	Pb [µg L^{-1}]	Rb [mg L^{-1}]	Sb [µg L^{-1}]	Si [mg L^{-1}]	Sr [mg L^{-1}]	Tl [µg L^{-1}]	U [µg L^{-1}]	V [µg L^{-1}]	Zn [µg L^{-1}]
BlPt Smoke	IS	15.43 (3.97)	<0.8 (1.69)	1.02 (9.21)	0.21 (0.20)	0.23 (<0.1)	4.57 (6.83)	13.26 (13.06)	<0.05 (0.23)	4.60 (3.34)	2.73 (8.25)	11.5 (36.3)
	HT	14.03 (0.67)										35.4 (58554)
Bott Sing	IS	0.8 (1.92)										<3 (6.82)
	HT	8.56 (0.68)										<3 (282)
Bott DwSt	IS	14.89 (-)										<3 (-)
H&C1	IS	27.41 (5.84)										<3 (<3)
	HT	8.10 (19.16)										13.5 (<3)
H&C2	IS	14.69 (17.81)										<3 (<3)
	HT	6.79 (9.43)	<0.8 (<0.8)	6.98 (11.05)	0.35 (0.39)	<0.1 (0.21)	124.30 (151.60)	13.01 (14.20)	0.12 (0.35)	1.28 (1.58)	1.65 (3.25)	3.19 (12)

Table 4.15 - List of trace elements detected in the interstitial (IS) fluids during the two MEFISTO campaigns in the cold seep system of the Trezze. Values between brackets refer to the April 2025 sampling campaign.

		Trace elements Fluids Trezze - Jul-24 (Apr-25)									
Site	Fluid	As [µg L^{-1}]	B [mg L^{-1}]	Ba [µg L^{-1}]	Br [g L^{-1}]	Cd [µg L^{-1}]	Cr [µg L^{-1}]	Cs [µg L^{-1}]	Fe [µg L^{-1}]	Li [mg L^{-1}]	Mn [µg L^{-1}]
SEPA	IS	5.83 (4.3)	6.38	22.07	0.12	0.37	0.98	0.73	<2	0.29	117.76 (9)
SUDPIASTRA	IS	4.5 (2.5)									5 (5)
SAN PIETRO	IS	1.5 (3.01)	(5.12)	(12.94)	(0.12)	(0.67)	(<0.5)	(0.61)	(39.50)	(0.26)	<4 (46.10)
Site	Fluid	Mo [µg L^{-1}]	Ni [µg L^{-1}]	Pb [µg L^{-1}]	Rb [mg L^{-1}]	Sb [µg L^{-1}]	Si [mg L^{-1}]	Sn [µg L^{-1}]	Sr [mg L^{-1}]	U [µg L^{-1}]	V [µg L^{-1}]
SEPA	IS	20.04 (12.)	2.10	<0.3	0.19	0.52	1.12	<1	12.61	4.25	9.87 (13.11)
SUDPIASTRA	IS	20. (20.)									8.80 (7.91)
SAN PIETRO	IS	17. (4.63)	(<0.5)	(0.63)	(0.19)	(0.35)	(1.45)	(1.36)	(11.85)	(3.56)	6.12 (6.85)

4.5. Sediments elemental composition

Elemental composition analyses carried out on the various sediment samples collected during the MEFISTO campaigns included total organic carbon (TOC) and total sulphur (TS). Table 4.16 resumes all the results obtained on sediments collected in Panarea during the March and September 2024 campaigns. In the samples collected from Panarea TOC ranged from 0.40 mgC g^{-1} (minimum detected in a sediment/biofilm sample collected in Hot & Cold2 Mar-24) and 129.56 mgC g^{-1}, value found for a biofilm sample collected in Bottaro Downstream in Sept-24. The lowest concentration of TS was detected in sediment samples from Zimmari (1.03 mgS g^{-1}), whereas the highest TS content was retrieved on a biofilm sample from Black Point Bubbling (632.29 mgS g^{-1}), both samples were collected during the March 2024 campaign.

Table 4.16 - Elemental analyses performed on the sediments during the MEFISTO Campaigns in Panarea; values are expressed per g of samples (mgC g^{-1} and mgS g^{-1}) and as percentage of dry weight of the sample (%C dw^{-1} and %S dw^{-1}). TOC - Total Organic Carbon, TS - Total Sulphur. Matrices: B - Biofilm; G - Gravel; P - Pebbles; F - Flocs; S - Sand. Values within square brackets refer to the September 2024 sampling.

Site	*Matrix*	TOC [mgC g^{-1}]	TOC [%C dw^{-1})]	TS [mgS g^{-1}]	TS [%S dw^{-1}]
		Mar-24 (Sept-24)			
Black Point Smoke	B	3.20	0.32	29.15	2.91
	G	(3.73)	(0.37)	(416.45)	(41.65)
	P				
Black Point Bubbling	B				
	F				
Bottaro Twins	B				
	G				
Bottaro Single	B				
	G				
	P				
Bottaro Downstream	B				
Hot & Cold1	S				
	B				
	G				
Hot & Cold1	S/B				
	S				
	S/B	0.40	0.04	1.79	0.18
Zimmari	S	1.04 (1.40)	0.1 (0.14)	1.03 (1.93)	0.1 (0.19)

The elemental composition of sediment samples collected in the cold seep system of the Trezze is summarised in Table 4.17. The data indicate a generally higher TOC and lower TS if compared with Panarea samples. The lowest TOC was found in SEPA during the July 2024 campaign (101.83 mgC g^{-1}) while the highest TOC concentration characterised SUDPIASTRA sediments in April 2025 (109.71 mgC g^{-1}). In Trezze, TS ranged between 0.58 mgS g^{-1} (BLANK Jul-24) and peaked in SAN PIETRO sediments sampled in July 2024 (2.23 mgS g^{-1}).

Table 4.17 - Elemental analyses performed on the sediments during the MEFISTO Campaigns in the cold seep system of the Trezze; values are expressed per g of dry sample (mgC g^{-1} and mgS g^{-1}) and as percentage of dry weight of the sample (%C dw^{-1} and %S dw^{-1}). TOC - Total Organic Carbon, TS - Total Sulphur. Matrices: S - Sediment. Values within square brackets refer to the April 2025 sampling.

Site	*Matrix*	TOC [mgC g^{-1}]	TOC [%C dw^{-1})]	TS [mgS g^{-1}]	TS [%S dw^{-1}]
		Jul-24 (Apr-25)			
SEPA	S	101.83 (105.68)	10.18 (10.57)	1.84 (0.81)	0.18 (0.09)
SUDPIASTRA	S	10			.20)
SAN PIETRO	S	10			.10)
BLANK	S	105.07 (103.01)	10.51 (10.30)	0.58 (0.64)	0.06)

4.6. Free gases

The results arising from the analysis of free gases completed during all the MEFISTO oceanographic campaigns are reported in Table 4.18. All Panarea sites showed minimal/trace content of He, H_2 and CO and no C_2H_6. CO_2 was the dominant gas over all the sites (range 93.53 - 98.73 %) followed by H_2S (range 0 - 5.27 %), N_2 (range 0.29 - 2.57 %), CH_4 (range 0 - 0.4845 %) and O_2 (range 0.0086 - 0.36 %).
Absence of CO and H_2S was recorded for the Trezze, whereas traces of He, H_2 and C_2H_6 could be detected in almost all the sites. Most abundant gases were CH_4 (range 76.59 - 90.2 %) followed by N_2 (4.86 - 21.41 %), CO_2 (0.13 - 4.19 %) and O_2 (0.0146 - 1.83 %). Apparently the gas sample from SAN PIETRO Jul-24 was contaminated from air, and it is reported in red in Tab 4.18.

Table 4.18 - Free gases composition analysis completed over the four MEFISTO oceanographic campaigns. Red: sample possibly contaminated by air.

Panarea Campaigns

Site	Sampling	He [%]	H2 [%]	O2 [%]	N2 [%]	CH4 [%]	CO [%]	CO2 [%]	H2S [%]	C2H6 [%]
BlackPoint	Mar-24	0.0008	0	0.0329	0.29	0.058	0	97.97	0.75	-
	Sept-24	0.0								-
Bottaro	Mar-24	0.00								-
	Sept-24	0.00								-
H&C	Mar-24	0.0								-
	Sept-24	0.0009	0	0.36	2.57	0.21	0	95.73	0	-

Trezze Campaigns

SEPA	Jul-24	0.0007	-	0.14	21.41	76.59	-	0.2	-	0.0061
	Apr-25	0.00								0.00073
SUDPIASTRA	Jul-24	0.0								0.0059
	Apr-25	0.00								-
SAN PIETRO	Jul-24	0.00								0.006
	Apr-25	0.00033	0.0007	1.83	15.4	82.28	-	0.28	-	0.00083

5. ACKNOWLEDGEMENTS

The MEFISTO research team would like to acknowledge the European Union that financially supported the project through the "Fund for the National Research Programme and Research Projects of Significant National Interest (PRIN)" in the framework of the NRRP - Next Generation EU Mission 4 "Education and Research". Thanks go to Captain Angelo Portelli and Captain Stefano Caressa for the logistical support provided by the vessels M/N Corvo and Castorino 2 during the activities conducted at sea. The MEFISTO research team would also like to thank Associate Professor Francesca Malfatti and Dr. Elena Peresani from the University of Trieste, who were in Panarea to take samples as part of the FEMTO project, and who were glad to make an intellectual and practical contribution to the MEFISTO activities. Special thanks goes to Dr. Valentina Esposito, Dr. Marco Graziano and Dr. Giuseppe De Rosa from OGS ECCSEL NatLab-Italy, who granted the access to the facility and enthusiastically supported the onshore laboratory activities, and to Shoreline cooperative company and Grado port authority for the logistical support provided during the campaigns in the Northern Adriatic Sea.

6. REFERENCES

Anzidei, M. and Esposito, A. (2003). New insights from high resolution bathymetric surveys in the Panarea volcanic complex (Aeolian Islands, Italy). In EGS-AGU-EUG Joint Assembly (p. 5923). http://www.cosis.net/abstracts/EAE03/05923/EAE03-J-05923.pdf

Anzidei, M. et al. (2005). The high resolution bathymetric map of the exhalative area of Panarea (Aeolian Islands, Italy). Annals of Geophysics. https://doi.org/10.4401/ag-3242

Becker, S. et al. (2020). GO-SHIP Repeat Hydrography Nutrient Manual: The Precise and Accurate Determination of Dissolved Inorganic Nutrients in Seawater, Using Continuous Flow Analysis Methods. Front. Mar. Sci. 7:581790. https://doi.org/10.3389/fmars.2020.581790

Bettoso, N. et al. (2023). Species richness of benthic macrofauna on rocky outcrops in the Adriatic Sea by using Species-Area Relationship (SAR) tools. Water, 15(2), 318. https://doi.org/10.3390/w15020318

Bockmon, E.E. and Dickson, A.G. (2014). A seawater filtration method suitable for total dissolved inorganic carbon and pH analyses. Limnology and Oceanography Methods Volume 12 (4) 191-195. https://doi.org/10.4319/lom.2014.12.191.

Boles, J. R. et al. (2001). Temporal variation in natural methane seep rate due to tides, Coal Oil Point area, California. Journal of Geophysical Research: Oceans, 106(C11), 27077-27086. https://doi.org/10.1029/2000JC000774

Calanchi, N. et al. (1999). Explanatory notes to the geological map (1: 10,000) of Panarea and Basiluzzo islands (Aeolian arc, Italy). Acta Vulcanologica, 11(2), 223-243.

Caliro, S. et al. (2004). Evidence of a recent input of magmatic gases into the quiescent volcanic edifice of Panarea, Aeolian Islands, Italy. Geophysical Research Letters, 31(7). L07619. https://doi.org/10.1029/2003GL019359

Cantoni, C. et al. (2012). Carbonate system variability in the gulf of Trieste (north Adriatic sea). Estuarine, Coastal and Shelf Science, 115, 51-62. https://doi.org/10.1016/j.ecss.2012.07.006

Capaccioni, B. et al. (2005). The November 2002 degassing event at Panarea Island (Italy): five months of geochemical monitoring. Annals of Geophysics. http://hdl.handle.net/2122/936

Capasso, G., Inguaggiato, S. (1998). A simple method for the determination of dissolved gases in natural waters. An application to thermal waters from Vulcano Island. Appl. Geochem. 13, 631–642.

Caracausi, A. et al. (2005). Changes in fluid geochemistry and physico-chemical conditions of geothermal systems caused by magmatic input: The recent abrupt outgassing off the island of

Panarea (Aeolian Islands, Italy). Geochimica et Cosmochimica Acta, 69(12), 3045-3059. https://doi.org/10.1016/j.gca.2005.02.011

Caressa, S. et al. (2001). Caratteri geomorfologici degli affioramenti rocciosi del Golfo di Trieste (Adriatico Settentrionale). Gortania Atti Museo Friulano di Storia Naturale, 23, 5-29.

Casellato, S. and Stefanon, A. (2008). Coralligenous habitat in the northern Adriatic Sea: an overview. Marine ecology, 29(3), 321-341. https://doi.org/10.1111/j.1439-0485.2008.00236.x

Ciais, P. et al. (2014). Carbon and other biogeochemical cycles. In Climate Change 2013: The Physical Science Basis. Contribution of Working Group I to the Fifth Assessment Report of the Intergovernmental Panel on Climate Change Change (pp. 465-570). Cambridge University Press.

Cossarini, G. et al. (2015). Spatiotemporal variability of alkalinity in the Mediterranean Sea. Biogeosciences, 12, 1647–1658. https//doi.org/10.5194/bg-12-1647-2015

Currie, K. et al. (2024). Determining Total Alkalinity. In K. Lowder, S. Chu, R. Easley, R. Spaulding, B. Peterson, K. Grabb, & A. Reed (Eds.), Practical Best Practices, version 1 (1st ed.). https://doi.org/10.21428/d8129fa3.1130d5cf

De Astis, G. et al. (2003). Geodynamic significance of the Aeolian volcanism (Southern Tyrrhenian Sea, Italy) in light of structural, seismological, and geochemical data. Tectonics, 22(4). https://doi.org/10.1029/2003TC001506

Di Bella et al. (2022). Potential resilience to ocean acidification of benthic foraminifers living in Posidonia oceanica Meadows: The case of the shallow venting site of Panarea. Geosciences, 12(5), 184. https://doi.org/10.3390/geosciences12050184

Dickson, A.G. et al. (2007)a. Guide to best practices on ocean CO2 measurements. Chapter 4 - Standard Operative Procedures SOP 1: Water sampling for the parameters of the oceanic carbon dioxide system. Picess Special Publication 3, IOCCP Report N8. https://www.ncei.noaa.gov/access/ocean-carbon-acidification-data-system/oceans/Handbook_2007/Guide_all_in_one.pdf

Dickson, A.G. et al. (2007)b. Guide to best practices on ocean CO2 measurements. Chapter 4 - Standard Operative Procedures SOP 2: Determination of total dissolved inorganic carbon in sea water. Picess Special Publication 3, IOCCP Report N8. https://www.ncei.noaa.gov/access/ocean-carbon-acidification-data-system/oceans/Handbook_2007/Guide_all_in_one.pdf

Dickson, A.G. et al. (2007)c. Guide to best practices on ocean CO2 measurements. Chapter 4 - Standard Operative Procedures SOP 3b: Determination of total alkalinity in sea water using an open-cell titration. Picess Special Publication 3, IOCCP Report N8. https://www.ncei.noaa.gov/access/ocean-carbon-acidification-data-system/oceans/Handbook_2007/Guide_all_in_one.pdf

Dickson, A.G. et al. (2007)d. Guide to best practices on ocean CO2 measurements. Chapter 4 - Standard Operative Procedures SOP 6b: Determination of the pH of sea water using the indicator dye m-cresol purple. Picess Special Publication 3, IOCCP Report N8. https://www.ncei.noaa.gov/access/ocean-carbon-acidification-data-system/oceans/Handbook_2007/Guide_all_in_one.pdf

Dickson, A. G. (2010). The carbon dioxide system in seawater: equilibrium chemistry and measurements. In Guide to best practices for ocean acidification research and data reporting, pp 17-52; Luxembourg: Publications Office of the European Union.

Dolfi, D. et al. (2007). Dome growth rates, eruption frequency and assessment of volcanic hazard: Insights from new U/Th dating of the Panarea and Basiluzzo dome lavas and pyroclastics, Aeolian Islands, Italy. Quaternary International, 162, 182-194. https://doi.org/10.1016/j.quaint.2006.05.035

Donda, F.et al. (2015). Deep-sourced gas seepage and methane-derived carbonates in the Northern Adriatic Sea. Basin research, 27(4), 531-545. https://doi.org/10.1111/bre.12087

Donda, F. et al. (2019). The origin of gas seeps in the Northern Adriatic Sea. Italian Journal of Geosciences, 138(2), 171-183. https://doi.org/10.3301/IJG.2018.34

Espa, S. et al. (2010). Field study and laboratory experiments of bubble plumes in shallow seas as analogues of sub-seabed CO2 leakages. Applied Geochemistry, 25(5), 696-704. https://doi.org/10.1016/j.apgeochem.2010.02.002

Esposito, A. et al. (2006). The 2002–2003 submarine gas eruption at Panarea volcano (Aeolian Islands, Italy): Volcanology of the seafloor and implications for the hazard scenario. Marine Geology, 227(1-2), 119-134. https://doi.org/10.1016/j.margeo.2005.11.007

Esposito, A. et al. (2010). Modeling ground deformations of Panarea volcano hydrothermal/geothermal system (Aeolian Islands, Italy) from GPS data. Bulletin of Volcanology, 72, 609-621. https://doi.org/10.1007/s00445-010-0346-y

Giani, M. et al. (2023). Elevated river inputs of the total alkalinity and dissolved inorganic carbon in the Northern Adriatic Sea. Water 15, 894. https://doi.org/10.3390/w15050894

Gordini E. (2009) - Integrazione di metodologie geofisiche, geomorfologiche, sedimentologiche e geochimiche per la definizione della genesi e dell'età degli affioramenti rocciosi presenti sul fondale marino dell'Adriatico settentrionale, (PhD's thesis). Retrieved from http://hdl.handle.net/10077/3206 . Trieste, IT: Univ. of Trieste.

Gordini, E. et al. (2012). Methane-related carbonate cementation of marine sediments and related macroalgal coralligenous assemblages in the Northern Adriatic Sea. In Seafloor Geomorphology as Benthic Habitat (pp. 185-200). Elsevier.

Gordini, E. et al. (2023). The role of methane seepage in the formation of the Northern Adriatic Sea geosites. Marine Geology, 462, 107081. https://doi.org/10.1016/j.margeo.2023.107081

Grasshoff, K. et al. (1999a). Methods of Seawater Analysis. 3rd Ed. Wiley-VCH, Weinheim (600 pp.).

Grasshoff, K. et al. (1999b). Methods of Seawater Analysis. 3rd Ed. Wiley-VCH, Weinheim (600 pp.).

Ingrosso, G. et al. (2016). Carbonate chemistry dynamics and biological processes along a river-sea gradient (Gulf of Trieste, Northern Adriatic Sea). Journal of Marine Systems 155, 35-49. http://dx.doi.org/10.1016/j.jmarsys.2015.10.013.

Ingrosso, G. et al. (2018). Mediterranean bioconstructions along the Italian coast. Advances in marine biology, 79, 61-136. https://doi.org/10.1016/bs.amb.2018.05.001

Inguaggiato, S., Rizzo, A. (2004). Dissolved helium isotope ratios in ground-waters: a new technique based on gas–water re-equilibration and its application to Stromboli volcanic system. Appl. Geochem. 19, 665–673.

Italiano, F. et al. (2009). Helium and carbon isotopes in the dissolved gases of Friuli region (NE Italy): geochemical evidence of CO_2 production and degassing over a seismically active area, Chem. Geol., 266, 76–85, https://doi.org/10.1016/j.chemgeo.2009.05.022, 2009.

Italiano, F. et al. (2014). Insights into mantle-type volatiles contribution from dissolved gases in artesian waters of the Great Artesian Basin, Australia, Chem. Geol., 378, 75–88, https://doi.org/10.1016/j.chemgeo.2014.04.013, 2014.

Jordan, S.F. et al. (2020). Bubble-mediated transport of benthic microorganisms into the water column: Identification of methanotrophs and implication of seepage intensity on transport efficiency. Scientific reports, 10(1), 4682. https://doi.org/10.1038/s41598-020-61446-9

Kirschke, S. et al. (2013). Three decades of global methane sources and sinks. Nature geoscience, 6(10), 813-823. https://doi.org/10.1038/ngeo1955

Langdon, C. (2010). Determination of dissolved oxygen in seawater by Winkler titration using the amperometric technique. The GO-SHIP Repeat hydrography Manual IOCCP report 14. http://www.go-ship.org/Manual/Langdon_Amperometric_oxygen.pdf

Lipej, L. et al. (2016). Biogenic Formations in the Slovenian Sea; National Institute of Biology. Marine Biology Station, Piran, 206p.

Liu, X. et al. (2011). Purification and Characterization of meta-Cresol Purple for Spectrophotometric Seawater pH Measurements. Environmental Science & Technology 2011 45 (11), 4862-4868. https://doi.org/10.1021/es200665d

Marchini, C. et al. (2021). Decreasing pH impairs sexual reproduction in a Mediterranean coral transplanted at a CO2 vent. Limnology and Oceanography, 66(11), 3990-4000. https://doi.org/10.1002/lno.11937

McGinnis, D.F. et al. (2006). Fate of rising methane bubbles in stratified waters: How much methane reaches the atmosphere?. Journal of Geophysical Research: Oceans, 111(C9). https://doi.org/10.1029/2005JC003183

Nieuwenhuize, J. et al.(1994). Rapid analysis of organic carbon and nitrogen in particulate materials. Mar. Chem. 45 (3), 217–224. https://doi.org/10.1016/0304-4203(94)90005-1

Nisbet, E.G. et al. (2019). Very strong atmospheric methane growth in the 4 years 2014–2017: Implications for the Paris Agreement. Global Biogeochemical Cycles, 33(3), 318-342. https://doi.org/10.1029/2018GB006009

Prather, M.J. et al. (2012). Reactive greenhouse gas scenarios: Systematic exploration of uncertainties and the role of atmospheric chemistry. Geophysical Research Letters, 39(9). https://doi.org/10.1029/2012gl051440

Pella, E., Colombo, B., (1973). Study of carbon, hydrogen and nitrogen determination by combustion-gas chromatography. Microchim. Acta 61 (5), 697–719. https://doi.org/10.1007/BF01218130

Romano, D. et al. (2019). Hazard scenarios related to submarine volcanic-hydrothermal activity and advanced monitoring strategies: A study case from the panarea volcanic group (aeolian islands, italy). Geofluids, 2019, 1-15. https://doi.org/10.1155/2019/8728720

Sani, T. et al. (2024). Ocean warming and acidification detrimentally affect coral tissue regeneration at a Mediterranean CO2 vent. Science of The Total Environment, 906, 167789. https://doi.org/10.1016/j.scitotenv.2023.167789

Saunois, M. et al. (2016). The global methane budget 2000–2012, Earth Syst. Sci. Data, 8, 697–751. https://doi.org/10.5194/essd-8-697-2016

Saunois, M. et al. (2020). The Global Methane Budget 2000–2017, Earth Syst. Sci. Data, 12, 1561–1623. https://doi.org/10.5194/essd-12-1561-2020

Saunois, M. et al (2025). Global methane budget 2000–2020. Earth System Science Data, 17(5), 1873-1958. https://doi.org/10.5194/essd-17-1873-2025

Shindell, D. et al. (2012). Simultaneously mitigating near-term climate change and improving human health and food security. Science, 335(6065), 183-189. https://doi.org/10.1126/science.1210026

Simson K. (2021). International Methane Emissions Observatory launched to boost action on powerful climate warming gas. International Methane Emissions Observatory, European Union.

Tassi et al. (2009). Low-pH waters discharging from submarine vents at Panarea Island (Aeolian Islands, southern Italy) after the 2002 gas blast: Origin of hydrothermal fluids and implications for volcanic surveillance. Applied Geochemistry, 24(2), 246-254. https://doi.org/10.1016/j.apgeochem.2008.11.015

Turicchia, E. et al. (2022). Bioconstruction and bioerosion in the northern Adriatic coralligenous reefs quantified by X-ray computed tomography. Frontiers in Marine Science, 8, 790869. https://doi.org/10.3389/fmars.2021.790869

Weber, T. et al. (2019). Global ocean methane emissions dominated by shallow coastal waters. Nature communications, 10(1), 4584. https://doi.org/10.1038/s41467-019-12541-7